Ocean Modelling 168 (2021) 101900

Contents lists available at ScienceDirect

Ocean Modelling

journal homepage: www.elsevier.com/locate/ocemod

Theory and analysis of acoustic-gravity waves in a free-surface compressible and stratified ocean

F. Auclair [a,*], L. Debreu [b], E. Duval [b], M. Hilt [a], P. Marchesiello [c], E. Blayo [b], F. Dumas [d], Y. Morel [c]

[a] Laboratoire d'Aérologie, Université de Toulouse, CNRS, UPS, France
[b] Univ. Grenoble Alpes, Inria, CNRS, Grenoble INP, LJK, 38000 Grenoble, France
[c] LEGOS, IRD, Université de Toulouse, CNRS, CNES, France
[d] Service Hydrographie et Océanographie de la Marine, Brest, France

ARTICLE INFO

Keywords:
Model of acoustic-gravity waves in the ocean
Free-surface compressible stratified ocean

ABSTRACT

Waves propagate in a free-surface ocean due to compressibility and gravity (and surface tension at much smaller scale). Analytical solutions have long been derived independently for acoustic and gravity waves, i.e., acoustic waves or internal-gravity waves in an unbounded ocean, surface-gravity waves in a free-surface-ocean, and acoustic or internal modes in a bounded ocean. In the present study, surface tension and earth-rotation are neglected and a simple, unified model based on inner and boundary dispersion relations is derived for waves propagating in a compressible, stratified, free-surface ocean. Branches of acoustic gravity wave solutions are identified and visually analysed in phase-space. Taylor developments are then carried out with respect to small parameters describing stratification and compressibility and are compared with numerical approximations of the intersection of inner and boundary dispersion surfaces. Finally, the model recovers the known approximations for swell, long-surface waves, internal-gravity waves, internal modes, acoustic waves or acoustic modes, and also provides information on the modifications of these solutions due to stratification and compressibility and on the coupling of acoustic and gravity waves. Two peculiar regions of the acoustic-gravity wave phase-space are more specifically highlighted and studied in detail: one for long waves shedding new light on the distinction between surface waves and low-order internal modes, the other for marginally stable surface waves of intermediate length-scale.

1. Introduction

Oceanographers have now access to high-performance numerical codes to explore and forecast the dynamics of a free-surface, compressible, non-hydrostatic ocean in a LES[1] context (Hilt et al., 2020; Marchesiello et al., 2021). Compressibility has not been reintroduced per se (acoustic waves remain at least a priori a nuisance for classical meso-scale configurations) but rather to avoid the resolution of large 3D numerical systems required to simulate non-hydrostatic dynamics under the Boussinesq assumption (Auclair et al., 2011, 2018). The compressible ocean codes are "local" (in the sens that the evolution of the dynamics at a point is only influenced by its neighborhood) and they are thus by nature well-adapted to massively-parallel processing; besides, computing costs can be drastically reduced by adjusting artificially the velocity of sound waves. Such an approach has already been implemented in weather forecasting models for nearly two decades (Skamarock et al., 2001) but several reasons can explain its late arrival in ocean modelling: the large gap between the velocities of ocean currents and sound waves but also the numerical treatment of the free-surface through time-splitting algorithms in ocean models (Shchepetkin and McWilliams, 2005) and the difficulty to adapt these algorithms to non-hydrostatic, compressible modelling (Auclair et al., 2018).

A much wider spectrum of acoustic-gravity waves (*AG waves*) can consequently be simulated numerically in realistic configurations of complex bathymetries, stratifications, forcing or ocean circulations raising fundamental questions not only about the dynamics itself of AG waves but also about their impact on low-frequency ocean circulation. Simple process-oriented ocean configurations are required to further explore the dispersion of AG waves and to evaluate the accuracy of their numerical representation in up-to-date ocean models. To achieve this, much can be learned from studying well-controlled propagations in laboratory water flumes: Dossmann et al. (2013) or Auclair et al. (2014) investigate for instance large internal waves induced above bathymetry simultaneously in laboratory and numerical configurations. More fundamental, analytical models remain nevertheless both necessary and essential. The objective pursued in this case is not only to

* Corresponding author.
E-mail address: francis.auclair@aero.obs-mip.fr (F. Auclair).

[1] For Large Eddy Simulation.

https://doi.org/10.1016/j.ocemod.2021.101900
Received 19 March 2021; Received in revised form 2 October 2021; Accepted 7 October 2021
Available online 26 October 2021
1463-5003/© 2021 Elsevier Ltd. All rights reserved.

document the propagation of AG waves in complex, realistic ocean configurations (numerical models are designed to do so) but also to treat fundamental, simple process-oriented configurations in order to gain a better understanding of the dynamics of AG waves and to provide simple solutions to evaluate the accuracy of numerical models. The present study is an original step in these directions.

Ocean AG waves cover a large variety of propagating mechanisms, and textbooks (LeBlond and Mysak, 1981; Gill, 1982; Pedlosky, 2013) have detailed the derivation of analytical solutions for decades. These waves can be classified in several categories depending on the type of mechanisms directly involved in their propagation. Neglecting Earth's rotation and associated planetary waves, two fundamental categories are of particular interest in the present study: acoustic (sound) waves, which are a consequence of ocean compressibility, and gravity waves, which are sustained by the gravity force. Table 1 gives a short (and necessarily incomplete) list of such waves. A particular type of waves is most often characterized by a space–time dispersion relation, linking its time frequency (or period) with its space wave-number (or wavelength). The phase and group velocities and wave dispersion capacity can be derived from the dispersion relations.

If ocean waves are short enough and generated far enough from surface and bottom boundaries, they can propagate in the ocean over a few wavelengths and during a few periods as in any unbounded medium. However, ocean waves can also take specific forms and propagate as *wave-modes* over the ocean *wave-guide*. For example, a stratified ocean is known to allow the propagation of internal gravity modes with "long" horizontal wavelengths compared to the ocean depth. Another example is given by the acoustic modes which are associated with compressibility effects (Jensen et al., 2011) and which have been recently revisited (Smith, 2015). Such internal and acoustic waves are qualified as "modes" because their vertical wavelength is constrained by the vertical extent of the domain. The ocean free-surface is permanently shaken by a myriad of horizontally propagating waves and it is not always clear whether these waves are modes or just "vertically-evanescent waves propagating horizontally". Capillary waves, swells, tidal waves, tsunamis are well-known examples of such free-surface waves.

Deriving a dispersion relation for acoustic waves or for internal waves in an unbounded ocean is rather straightforward. The method generally includes two steps: small amplitude is assumed; only specific wave-restoring mechanisms and medium characteristics are retained in the simplest possible wave dispersion model (compressibility and pressure force for acoustic waves, gravity and vertical advection of isopycnal surfaces for internal waves) (Lighthill, 1967).

The introduction of a free-surface brings more complexity. Small-amplitude is postulated in this case also and both gravity and free-surface motions are retained in the dispersion model. Surface waves are "edge waves" propagating at the interface between the atmosphere and the ocean, and the surface kinematic relation (the free-surface general boundary condition) leads to a transcendental dispersion relation with trigonometric terms. As a result, further simplifications are needed and specific analytical solutions can then be found in the literature depending, for example, on relative depth, i.e., the product of horizontal wave-number k_x and ocean depth H (Table 1). Long gravity waves are particular solutions of small aspect ratio $k_x H$, well-known to propagate horizontally with $\sqrt{gH}$ phase and group velocities (where g is the acceleration of gravity and H a reference depth). Interestingly enough, such waves occur in at least two distinct contexts. Shallow-water waves (SHW) are propagating solutions of shallow-water models, their vertical wave-length is then viewed as infinite (much larger than their horizontal wave-length). Long swells (LSW) are also propagating with the same phase and group velocities but, in this case, they retain some of the properties of swells and their horizontal and vertical wave-lengths have similar magnitudes.

SHW and LSW are often considered as similar since their wave velocity (Ω/k_x) are equal. However due to the underlying assumptions made in the models leading to these solutions, LSW horizontal and vertical wave-numbers have equal absolute values ($|k_{z,lsw}| = |k_x|$) whereas SHW have a vanishing vertical wave-number ($k_{z,shw} = 0$).

Dukowicz (2013) tackled the description of AG waves and proposed a review of *"Various approximations in atmosphere and ocean models based on an exact treatment of gravity wave dispersion"*. In that paper, acoustic-gravity waves were shown to satisfy a system of two dispersion relations and the impact of several usual assumptions of ocean models was evaluated. The present study builds on Eckart (1960) and Dukowicz (2013)'s results and more specifically focuses on the impact of both stratification and compressibility on AG-wave solutions in the ocean. The objective is not to provide a full description of AG waves in any realistic configurations (up-to-date numerical models being developed for this) but rather to focus on a simple and classical configuration leading to a unified, as-general-as-possible, analytical model. Taylor expansions of dispersion relations and resulting expressions for wavelength and frequency are more systematically derived in terms of compressibility and stratification. Surface waves are systematically studied together with internal and acoustic modes. Long-wave solutions are investigated here in detail. Another original aspect of the present study is that acoustic modes are discussed in the frame of classical ocean acoustics (Jensen et al., 2011) and additional "poles" (singularities) of the dispersion relations induced by stratification and gravity are found. A peculiar region of phase-space is also identified where surface acoustic-gravity surface wave are "marginally stable" and gravity and compressibility are both important. To the authors knowledge, the existence of such a region has never been discussed in the literature. A graphic analysis of wave solutions is proposed in 3D frequency/wave-number phase-space, unfolding their dependency on the vertical wave-number.

In the Section 2, a linear model of ocean wave propagation is proposed with bottom and surface boundary conditions, and a system of two dispersion relations (the *inner* and *boundary* dispersion relations) is derived. The inner dispersion relation and the wave solutions propagating in an unbounded ocean are studied in detail in Section 3. Waves propagating in a bounded ocean are investigated in Section 4 and conclusions are drawn in Section 5.

2. Linear model for surface and internal acoustic-gravity waves

2.1. General model for a compressible, viscous ocean

Ocean dynamics can be described with a small number of macroscopic variables: velocity ($\mathbf{v}$), pressure and density (p and ρ), temperature and salinity (T and S). The general equations governing the motion of a compressible, viscous ocean are then:

$$\frac{\partial \rho}{\partial t} = -\nabla \cdot (\rho \mathbf{v}) \tag{1a}$$

$$\frac{\partial \rho \mathbf{v}}{\partial t} = -\nabla \cdot (\rho \mathbf{v} \otimes \mathbf{v}) - 2\rho\, \boldsymbol{\Omega} \times \mathbf{v} - \nabla p + \nabla \cdot \left(\mu(\nabla \mathbf{v} + \nabla \mathbf{v}^{\,T}) + \mu_2 (\nabla \cdot \mathbf{v})\, \mathbf{I} \right) + \rho \mathbf{g} \tag{1b}$$

$$\frac{\partial \rho T}{\partial t} = -\nabla \cdot (\rho T \mathbf{v}) + \nabla \cdot (\kappa_T \nabla T) \tag{1c}$$

$$\frac{\partial \rho S}{\partial t} = -\nabla \cdot (\rho S \mathbf{v}) + \nabla \cdot (\kappa_S \nabla S) \tag{1d}$$

$$\rho = \rho(T, S, p) \tag{1e}$$

where $\mathbf{I}$ is the identity matrix, superscript T indicates transposition, μ and μ_2 are the kinetic and bulk (or second) viscosities, $\boldsymbol{\Omega}$ is earth angular velocity, κ_T and κ_S are the heat and salt diffusivities. These equations are written in a conservative form. They specify basic conservation principles: conservation of mass for Eq. (1a), conservation of momentum for Eq. (1b) and conservation of heat and salt for Eqs. (1c) and (1d). Eq. (1e) is a functional relation describing the thermodynamic equation of state (EOS).

At the bottom ($z = -H$) and surface ($z = \zeta$) of the ocean, boundary conditions must be specified for each variable (or for its derivatives). A

Table 1
Simplified models of ocean waves and modes and their dispersion relations in a vertical section, for an unbounded ocean (top) and for a bounded ocean (bottom). Ω is the angular frequency of the wave, k_x and k_z are the horizontal and vertical wave-numbers, g is the acceleration of gravity, H a reference depth, N a reference Brunt-Väisälä angular frequency and c_s the speed of sound. n and m are two strictly positive integer numbers.

Waves	Assumptions	Angular frequency(Ω)	Vertical wave-number (k_z)
Acoustic waves	Compressible, unbounded	$\Omega_{aw}^2 = c_s^2(k_x^2 + k_z^2)$	Independent
Internal gravity waves	Stratified, unbounded	$\Omega_{igr}^2 = \dfrac{N^2 k_x^2}{k_x^2 + k_z^2}$	Independent
Acoustic gravity modes	Compressible, bounded	$\Omega_{am}^2 = c_s^2(k_x^2 + k_z^2)$	$k_{z,am} = \dfrac{\pi}{2H} + \dfrac{m\pi}{H}$
Swell	Free-surface	$\Omega_{sw}^2 = gk_x \tanh(k_x H)$	$\lvert k_{z,sw}\rvert = \lvert k_x\rvert$
Swell (long)	Free-surface	$\Omega_{lsw}^2 = gH\ k_x^2$	$\lvert k_{z,lsw}\rvert = \lvert k_x\rvert$
Shallow water waves	Free-surface, shallow	$\Omega_{shw}^2 = gH\ k_x^2$	$k_{z,shw} = 0$
Internal gravity modes	Stratified, bounded	$\Omega_{im}^2 = \dfrac{N^2 k_x^2}{k_x^2 + k_z^2}$	$k_{z,im} = \dfrac{n\pi}{H}$

simple condition of no penetration and no-slip at the ocean flat-bottom can be written:

$$\mathbf{v}(\mathbf{x_H}, z = -H, t) = \mathbf{0} \tag{2}$$

In an inviscid flow, this latest relation is that of no normal velocity. Neglecting surface-tension pressure drop, surface pressure is given by:

$$p(\mathbf{x_H}, z = \zeta, t) = p_{atm} \tag{3}$$

with p_{atm} the atmospheric pressure imposed at the surface of the ocean. Surface capillarity waves are consequently filtered out and will be neglected in the remaining of this work.

Relation (2) corresponds to Jensen et al.'s "hard-bottom condition" with no propagation nor penetration of acoustic waves in sediment and geologic layers beneath the ocean floor (Jensen et al., 2011). The authors additionaly recover Relation (3) by assuming that the atmosphere behaves as a vacuum medium for acoustic waves. This means that acoustic waves propagating from the ocean toward the ocean floor or toward the atmosphere are integrally reflected back to the ocean.

The surface kinematic condition expresses the motion of the free-surface and relates the free-surface displacement ζ to the surface vertical velocity w:

$$\frac{\mathrm{d}\zeta(\mathbf{x_H}, t)}{\mathrm{dt}} = w(\mathbf{x_H}, z = \zeta, t) \tag{4}$$

This kinematic boundary condition allows the propagation of surface gravity waves.

2.2. EOS based on pressure and density decomposition

Waves are defined as small disturbances to a motionless thermodynamic equilibrium state, and both pressure and density can be decomposed into an equilibrium component and a small increment. In addition, as a first approximation, the impact of atmospheric pressure p_{atm} can be neglected — it can take an active part in wave generation, but only plays a minor role during propagation.

The usual decomposition is now formalized for pressure (5a) and density (5b):

$$\begin{aligned} p(\mathbf{x}, t) &= \underbrace{\underbrace{p_{atm}(\mathbf{x_H}, t)}_{\approx 0} + g\int_z^\zeta \rho_h(\mathbf{x_H}, z', t)\ dz'}_{p_h(\mathbf{x},t)} + \delta p(\mathbf{x}, t) \\ &= \underbrace{\underbrace{g\int_z^\zeta \hat{\rho}_h(z')\ dz'}_{\hat{p}_h(z)} + \underbrace{g\int_z^\zeta \left(\rho_h(\mathbf{x_H}, z', t) - \hat{\rho}_h(z')\right)\ dz'}_{p'_h(\mathbf{x},t)}}_{p_h(\mathbf{x},t)} + \delta p(\mathbf{x}, t) \end{aligned} \tag{5a}$$

$$\begin{aligned} \rho(\mathbf{x}, t) &= \underbrace{\hat{\rho}_{TS}(z) + \rho'_{TS}(\mathbf{x}, t)}_{\rho_{TS}(\mathbf{x},t) = \rho(T,S,p=0)} + \underbrace{\frac{1}{c_s^2}\left(\hat{p}_h(z) + p'_h(\mathbf{x}, t) + \delta p(\mathbf{x}, t)\right)}_{\partial\rho/\partial p|_{T,S}\ \ p(\mathbf{x},t)} + \mathrm{O}(p^2) \\ &\approx \underbrace{\underbrace{\hat{\rho}_{TS}(z) + \frac{\hat{p}_h(z)}{c_s^2}}_{\approx\hat{\rho}_h(z)} + \underbrace{\rho'_{TS}(\mathbf{x}, t) + \frac{p'_h(\mathbf{x}, t)}{c_s^2}}_{\rho'_h(\mathbf{x},t)}}_{\approx\rho_h(\mathbf{x},t)} + \frac{\delta p(\mathbf{x}, t)}{c_s^2} \end{aligned} \tag{5b}$$

with $\partial\rho/\partial p|_{T,S} = c_s^2$ at constant temperature and salinity, $\partial\hat{p}_h/\partial z = -\hat{\rho}_h(z)g$, $\partial p'_h/\partial z = -\rho'_h(z)g$. The first decomposition $p = p_h + \delta p$ is defined by an hydrostatic component p_h and a nonhydrostatic pressure increment δp. It is based on a division of the pressure field into a slow varying component in hydrostatic equilibrium and a fast varying nonhydrostatic component. Density can then be obtained from the EOS (1e) and a first-order Taylor development is carried out for small total pressure. Its Lagrangian evolution can be directly related to the Lagrangian evolution of pressure under the assumption of heat and salt conservation ($d\rho_{TS}/dt = 0$) when both heat and salt diffusions can be neglected:

$$\frac{\mathrm{d}\rho}{\mathrm{dt}} = \frac{\mathrm{d}\rho_{TS}}{\mathrm{dt}} + \frac{1}{c_s^2}\frac{\mathrm{d}p}{\mathrm{dt}} = \frac{1}{c_s^2}\frac{\mathrm{d}p}{\mathrm{dt}} \tag{6}$$

The Brunt-Väisälä frequency for a compressible ocean (Gill, 1982, p169) is defined by:

$$N^2 = -g/\hat{\rho}_h(z)\partial\hat{\rho}_h/\partial z - g^2/c_s^2 \tag{7}$$

Note that $\hat{\rho}_h(z)$ includes compressibility effects but not N^2 and that, in (5b), we made the further assumption that:

$$\rho_{TS} + \frac{p_h}{c_s^2} \approx \rho_h = \hat{\rho}_h + \rho'_h \tag{8}$$

This relation is indeed an approximation since the non-hydrostatic component of density, leading for instance to convective instabilities, has been neglected at the right-hand-side.

Relations (5a), (5b), (6) and (8) are central to the derivation of the present model of AG waves, they also provide the basis for a rather complete analysis to identify and evaluate the approximations made in more realistic, compressible, non-hydrostatic, free-surface numerical models of the ocean.

2.3. Linear inviscid, non-rotating wave model

In the following, ocean is supposed to remain flat-bottomed, Coriolis pseudo-force is neglected and viscosities and diffusivities μ, μ_2, κ_T and κ_S are vanishing in an inviscid ocean. Combining mass conservation (1a) and equation of state (6):

$$-\rho\nabla\cdot\mathbf{v} = \frac{1}{c_s^2}\frac{\mathrm{d}p}{\mathrm{dt}} \tag{9}$$

Without loss of generality, the present study can now be restricted to the (O, x, z) vertical plane (O being the origin) to simplify notations. Eq. (9) can then be expanded to:

$$-\rho\left(\frac{\partial u}{\partial x} + \frac{\partial w}{\partial z}\right) = \frac{1}{c_s^2}\left(\frac{\partial p}{\partial t} + u\frac{\partial p}{\partial x} + w\frac{\partial p}{\partial z}\right) \tag{10}$$

A Taylor expansion of model equations can now be carried out in the vicinity of the reference profiles $(\hat{\rho}_h(z),\ \hat{p}_h(z))$ and of a resting fluid $(u = w = 0)$. Small amplitude wave-induced increments are given by $\delta V = (p'_h + \delta p,\ \rho'_h + \delta p/c_s^2,\ u,\ w)$. At first order in δV, conservation of mass and vertical advection of pressure and density can be rewritten. The left-hand side of (10) becomes:

$$-\rho\left(\frac{\partial u}{\partial x} + \frac{\partial w}{\partial z}\right) = -\left(\frac{\partial \hat{\rho}_h u}{\partial x} + \frac{\partial \hat{\rho}_h w}{\partial z} - w\frac{\partial \hat{\rho}_h}{\partial z}\right) + \mathrm{O}(\delta V^2)$$

while the right-hand side of (10) becomes:

$$\frac{1}{c_s^2}\left(\frac{\partial p}{\partial t} + u\frac{\partial p}{\partial x} + w\frac{\partial p}{\partial z}\right) = \frac{1}{c_s^2}\left(\frac{\partial p}{\partial t} + w\frac{\partial \hat{p}_h}{\partial z}\right) + \mathrm{O}(\delta V^2)$$
$$= \frac{1}{c_s^2}\left(\frac{\partial p}{\partial t} - \hat{\rho}_h g w\right) + \mathrm{O}(\delta V^2)$$

leading to:

$$\frac{\partial p}{\partial t} = -c_s^2\left(\frac{\partial \hat{\rho}_h u}{\partial x} + \frac{\partial \hat{\rho}_h w}{\partial z}\right) + \underbrace{\left(g + \frac{c_s^2 \partial \hat{\rho}_h(z)/\partial z}{\hat{\rho}_h(z)}\right)}_{-c_s^2 N^2/g}\hat{\rho}_h w + \mathrm{O}(\delta V^2) \tag{11}$$

At first order in δV, pressure at $z = 0$ can be related to the free-surface displacement through the hydrostatic relation:

$$p(z=0) = \hat{\rho}_h(0) g\zeta + \mathrm{O}(\delta V^2) \tag{12}$$

and the kinematic boundary condition can be rewritten for pressure:

$$\frac{\partial p}{\partial t}(z=0) = g\hat{\rho}_h(0) w(z=0) + \mathrm{O}(\delta V^2) \tag{13}$$

Based on the pressure and density decomposition proposed in Section 2.2, a simpler, inviscid, linear, rotation-free $p-\rho$ model can be used to model acoustic, internal and surface waves. At first order in wave-induced increment δV, the conservation of momentum and mass and the EOS read:

$$\frac{\partial \hat{\rho}_h u}{\partial t} = -\frac{\partial p}{\partial x} \tag{14a}$$
$$\frac{\partial \hat{\rho}_h w}{\partial t} = -\frac{\partial p}{\partial z} - \rho g \tag{14b}$$
$$\frac{\partial \rho}{\partial t} = -\left(\frac{\partial \hat{\rho}_h u}{\partial x} + \frac{\partial \hat{\rho}_h w}{\partial z}\right) \tag{14c}$$
$$\frac{\partial p}{\partial t} = -c_s^2\left(\frac{\partial \hat{\rho}_h u}{\partial x} + \frac{\partial \hat{\rho}_h w}{\partial z}\right) - \overbrace{\left(\frac{c_s^2}{D(z)} - g\right)}^{c_s^2 N^2/g}\hat{\rho}_h w \tag{14d}$$

with the (flat) bottom condition (under the inviscid flow assumption) and the surface condition:

$$w(z=-H) = 0 \tag{15a}$$
$$\frac{\partial p}{\partial t}(z=0) = \hat{\rho}_h\, g\, w(z=0) \tag{15b}$$

Following Dukowicz (2013), a vertical length scale (written $D(z)$) associated with stratification is defined by $D(z) = -\dfrac{\hat{\rho}_h(z)}{\partial \hat{\rho}_h(z)/\partial z} = 1/\left(\dfrac{N^2(z)}{g} + \dfrac{g}{c_s^2}\right)$.

2.4. General propagation equation and polarization

Form of wave solutions. Dispersion relations can be derived by postulating and specifying the wave form. Horizontally-propagating surface waves, wave modes propagating in the ocean wave guide, internal waves and acoustic waves all satisfy the following "polarization" relations:

$$\begin{pmatrix} \hat{\rho}_h u \\ \hat{\rho}_h w \\ \rho \\ p \end{pmatrix} = \begin{pmatrix} \widetilde{U}(z) \\ \widetilde{W}(z) \\ \widetilde{\rho}(z) \\ \widetilde{p}(z) \end{pmatrix} e^{i(k_x x - \Omega t)} \tag{16}$$

where k_x and Ω are respectively the horizontal wave-number and wave frequency.

Inner propagation equation & polarization. The polarization relations (16) can then be substituted in the propagation model (14a)–(14d) and in the bottom boundary conditions (15a) to obtain a homogeneous system of 4 equations with 4 unknowns. The vertical profiles $\widetilde{U}(z)$, $\widetilde{\rho}(z)$ and $\widetilde{p}(z)$ can eventually be expressed in terms of $\widetilde{W}(z)$ to obtain an ordinary differential equation for $\widetilde{W}(z)$:

$$\widetilde{W}''(z) + \frac{1}{D(z)}\widetilde{W}'(z) + \left(k_x^2\frac{N^2-\Omega^2}{\Omega^2} + \frac{\Omega^2}{c_s^2} - \frac{D'(z)}{D^2(z)}\right)\widetilde{W}(z) = 0 \tag{17}$$

Assuming for now that $\Omega^2 \neq c_s^2 k_x^2$ (this particular case is studied in Section 2.6), the following polarization relations must be satisfied:

$$\widetilde{U}(z) = -ik_x\,\frac{(c_s^2 - gD(z))\,\widetilde{W}(z) + c_s^2 D(z)\,\widetilde{W}'(z)}{D(z)\,(\Omega^2 - c_s^2 k_x^2)} \tag{18a}$$
$$\widetilde{\rho}(z) = -i\,\frac{k_x^2\,(c_s^2 - gD(z))\,\widetilde{W}(z) + \Omega^2 D(z)\widetilde{W}'(z)}{D(z)\,\Omega\,(\Omega^2 - c_s^2 k_x^2)} \tag{18b}$$
$$\widetilde{p}(z) = -i\Omega\,\frac{(c_s^2 - gD(z))\,\widetilde{W}(z) + c_s^2 D(z)\,\widetilde{W}'(z)}{D(z)\,(\Omega^2 - c_s^2 k_x^2)} \tag{18c}$$

Boundary dispersion relations. The polarization relations must also be substituted in the surface boundary condition (15b), leading to:

$$-i\Omega\,\widetilde{p}(0) = g\widetilde{W}(0) \tag{19}$$

or, using (18),

$$\widetilde{W}'(0) + \left(\frac{1}{D(0)} - \frac{gk_x^2}{\Omega^2}\right)\widetilde{W}(0) = 0 \tag{20}$$

Note that this differs from the surface boundary condition usually found in textbooks (e.g. Gill, 1982) is given by

$$\widetilde{W}'(0) - \left(\frac{gk_x^2}{\Omega^2}\right)\widetilde{W}(0) = 0. \tag{21}$$

Eq. (20) is identical to equation 71 of Dukowicz (2013) but is obtained in an Eulerian framework.

The boundary condition at the ocean floor is given by:

$$\widetilde{W}(-H) = 0. \tag{22}$$

Change of variables. First-order terms can be removed in the ordinary differential equation (17) and further developments can be simplified by making the following change of variable:

$$\widetilde{W}(z) = \widetilde{W}(0)\,F(z)\,e^{\int_z^0 \frac{dz'}{2D(z')}} \tag{23}$$

with $F(0) = 1$. Substituting this relation in (17) leads to a second-order ordinary differential equation for the unknown function $F(z)$:

$$F''(z) + \left(k_x^2\frac{N^2-\Omega^2}{\Omega^2} + \frac{\Omega^2}{c_s^2} - \frac{1+2D'(z)}{4D(z)^2}\right)F(z) = 0 \tag{24}$$

$F(z)$ differs from the vertical momentum profile $\widetilde{W}(z)$ by the attenuation factor $\exp\left(\int_z^0 \frac{dz'}{2D(z')}\right)$. This factor reduces the vertical extent of wave anomalies based on the length scale $D(z)$. The weaker the stratification, the larger $D(z)$ and the closer to each other the vertical velocities $\widetilde{W}(z)$ and $F(z)$.

Boundary dispersion relation. In terms of the unknown function $F(z)$, the surface and bottom boundary conditions ((20) and (22)) reads:

$$F'(0) + \left(\frac{1}{2D(0)} - \frac{gk_x^2}{\Omega^2}\right)F(0) = 0 \tag{25a}$$
$$F(-H) = 0 \tag{25b}$$

Constant brunt-väisälä frequency. In the remaining of the paper, the Brunt-Väisälä frequency is assumed to be constant: $N^2(z) = N_0^2$, or equivalently $D(z) = D_0$. Eq. (23) can then be rewritten:

$$\widetilde{W}(z) = \widetilde{W}(0)\, e^{-z/2D_0}\, F(z) \tag{26}$$

and $\hat{\rho}_h(z)$ is given by $\hat{\rho}_h(z) = \hat{\rho}_h(0)\, e^{-z/D_0}$. The general expression of the vertical velocity perturbation profile for a constant scale height D_0 is thus:

$$w(x,z,t) = \frac{1}{\hat{\rho}_h(z)}\widetilde{W}(z)\, e^{i(k_x x - \Omega t)} = \frac{\widetilde{W}(0)}{\hat{\rho}_h(0)}\, e^{-z/2D_0}\, F(z)\, e^{i(k_x x - \Omega t)} \tag{27}$$

Leaving aside for now the surface boundary condition, the vertical profile $F(z)$ has to satisfy the following system of equations:

$$F''(z) + \overbrace{\left(k_x^2 \frac{N_0^2 - \Omega^2}{\Omega^2} + \frac{\Omega^2}{c_s^2} - \frac{1}{4D_0^2}\right)}^{\equiv k_z^2} F(z) = 0 \tag{28a}$$

$$F(-H) = 0 \tag{28b}$$

The general solution of (28a)–(28b) with the normalization $F(0) = 1$ is

$$F(z) = \frac{\sin\left(k_z(H+z)\right)}{\sin(k_z H)} \tag{29}$$

where the vertical wave-number k_z is defined in (28a) and is a function of k_x and Ω. Note that $F(z)$ is linear for $k_z = 0$, this particular case will be considered separately in Section 2.6.

2.5. Inner and boundary dispersion relations

The relation introduced in (28a) between the vertical wave-number k_z, horizontal wave-number k_x and wave frequency Ω constitutes the first dispersion relation. It is rewritten as:

$$k_z^2 + k_x^2\left(1 - \frac{N_0^2}{\Omega^2}\right) - \frac{\Omega^2}{c_s^2} + \frac{1}{4D_0^2} = 0 \tag{30}$$

This relation does not account for surface or bottom boundary conditions and thus only deals with the propagation of waves in the inner ocean. It will now be referred to as the *inner dispersion relation*. The bottom boundary condition is accounted for in the general solution profile given by (29). Injecting this vertical profile $F(z)$ into the surface boundary condition (28a) then leads to the *boundary dispersion relation*:

$$\Omega^2 = \frac{g k_x^2 \tan(H k_z)}{k_z + \frac{\tan(H k_z)}{2D_0}} = \frac{g k_x^2}{\frac{1}{2D_0} + k_z \operatorname{cotan}(H k_z)} \tag{31}$$

A wave propagating in a "bounded ocean" must satisfy both the *inner* and *boundary dispersion relations* (30) and (31). Note that the traditional inner and boundary dispersion relations for a Boussinesq, incompressible fluid (Gill, 1982, Table 1) can be recovered from (30) and (31) by setting $c_s \to +\infty$ (incompressibility) and then $D_0 \to +\infty$ (incompressibility and Boussinesq approximations), leading to:

$$\begin{aligned} &k_z = k_{z,im} = \frac{n\pi}{H} \quad \text{and} \\ &\Omega^2 = \Omega_{im}^2 = N^2 \frac{k_x^2}{k_x^2 + k_z^2} = g k_x^2 \frac{\tan(H k_z)}{k_z} \quad \text{for} \quad n \in \mathbb{N}^* \end{aligned} \tag{32}$$

Dimensionless dispersion relations. As in Dukowicz (2013), several parameters are now defined to obtain dimensionless dispersion relations:

$$\epsilon_i^2 = \frac{N^2 H}{g}, \quad \epsilon_a^2 = \frac{gH}{c_s^2} \quad \text{and} \quad \epsilon^2 = \frac{\epsilon_i^2 + \epsilon_a^2}{2} = -\frac{H}{\hat{\rho}_h(z)}\frac{\partial \hat{\rho}_h}{\partial z} \tag{33}$$

ϵ_i is thus a small parameter related to gravity, defined as the ratio of the order of magnitude of the first internal mode "NH" velocity to the velocity of long surface waves $\sqrt{gH}$. ϵ_a is a small parameter related to acoustics, defined as the ratio of the speed of long surface waves $\sqrt{gH}$ to that of sound waves c_s. Note that ϵ_i is defined based on Brunt-Väisälä frequency N (7) to which compressibility effects (g^2/c_s^2 term) have been subtracted whereas ϵ refers to an equivalent stratification where the effects of compressibility are included. In a homogeneous ocean, ϵ_i vanishes when $N \approx 0$. The depth scale can then be rewritten as: $D_0 = 2H/\epsilon^2$. This scale-depth does not include any compressibility-induced correction. As a consequence the ratio $H/D_0 = 2\epsilon^2$ gives an idea of the relative strength of the ocean stratification.

Three dimensionless variables are also further defined:

$$\omega = \Omega\sqrt{\frac{H}{g}}, \quad \delta_x = k_x H, \quad \delta_z = k_z H \tag{34}$$

The inner (30) and boundary (31) dispersion relations can be written in terms of the dimensionless parameters and variables as:

$$\delta_x^2 + \delta_z^2 = \epsilon_i^2 \frac{\delta_x^2}{\omega^2} + \epsilon_a^2 \omega^2 - \epsilon^4 \tag{35a}$$

$$\omega^2 = \frac{\delta_x^2 \tan(\delta_z)}{\delta_z + \epsilon^2 \tan(\delta_z)} \tag{35b}$$

In a free-surface ocean, wave solutions must satisfy simultaneously relations (35a) and (35b). This means that only one parameter among the frequency ω and horizontal or vertical wave-numbers (δ_x and δ_z) can be imposed. For short vertical wave numbers and far from the bottom and surface boundaries, wave solutions only need to satisfy the inner dispersion relation to be dynamically consistent. Pure acoustic waves or pure internal-gravity waves are known to propagate in the inner ocean as in an unbounded ocean.

The resulting set of two Eqs. (35a)–(35b) for the three variables (δ_x, δ_z, ω) and the two parameters ϵ_a, ϵ_i is nonlinear, and simple general solutions cannot be found analytically.

2.6. Acoustic Lamb waves & depth-independent surface gravity waves

Acoustic lamb waves. The polarization relations (18) have been derived after excluding the particular dispersion relation:

$$\epsilon_a^2 \omega^2 = \delta_x^2 \tag{36}$$

which is the dispersion relation for acoustic Lamb waves (for atmospheric Lamb waves see for instance Apel, 1987). To be a solution of the linear inviscid, non-rotating wave model (14a)–(14d) with bottom boundary condition (15a), these waves must be of the form:

$$\left(\widetilde{W}(z),\ \widetilde{p}(z),\ \widetilde{U}(z),\ \widetilde{\rho}(z)\right) = p_0\left(0,\ 1,\ 1/c_s,\ 1/c_s^2\right)\ e^{-gz/cs^2} \tag{37}$$

Surface pressure must then vanish to satisfy the surface boundary condition (15b) which can only be obtained for the trivial null solution ($p_0 = 0$).

This does not mean that Lamb waves cannot propagate in the real ocean but just that they are not solutions of the present ocean model (Section 2.3) due to the surface and bottom boundary conditions: indeed to have non-zero amplitude, the pressure (or alternatively the vertical velocity) must vanish simultaneously at the surface and at the ocean floor. A vanishing pressure both at the surface and at the ocean floor can for instance be found in Jensen's formulation of Pekeris wave guide (Jensen et al., 2011) whereas a vanishing vertical velocity can alternatively be specified by assuming that the present linear inviscid, non-rotating wave model is also rigid lid: (15b) is then replaced by $w(z=0) = 0$. In this case, the wave polarization is given by (37) with p_0 the pressure at the surface of the ocean.

Depth-independent surface gravity wave. A second interesting wave solution has been identified in Section 2.4 for $\delta_z = \delta_{z,0} = 0$. Indeed $F(z)$ is then a linear function of z which simplifies to $F(z) = (z+H)/H$

to satisfy the bottom boundary condition (28b). The surface boundary condition (35b) and the inner dispersion relation (35a) impose that:

$$\omega^2 = \omega_0^2 = \frac{\delta_{x,0}^2}{1+\epsilon^2},$$
$$\delta_x^2 = \delta_{x,0}^2 = \frac{(1+\epsilon^2)(\epsilon_i^2+\epsilon^2(\epsilon_i^2-\epsilon_a^2)/2)}{1+(\epsilon_i^2-\epsilon_a^2)/2} = \epsilon_i^2 + O(\epsilon_i^4, \epsilon_a^4) \tag{38}$$

This wave can only propagate at a well-defined long horizontal wavelength $\delta_x = \delta_{x,0}$ which vanishes in a homogeneous ocean ($\epsilon_i = 0$). It is also depth-independent since if vertical wave-number vanishes.

This depth-independent surface gravity wave presents similarities with Lamb waves (36). Both solutions are found as particular cases while deriving the polarization relations for acoustic-gravity waves and they are associated with a horizontally-propagating convergent-divergent motion of the water column (a depth-independent motion of this water column compensated by a displacement of the free-surface). This motion is induced by gravity for depth-independent surface gravity waves and by compressibility for Lamb waves.

2.7. Frequency is real & vertical wave-number is either real or imaginary

Based on (24) and on the boundary conditions (25a) and (25b), the vertical wave-number δ_z can be shown to be either real or imaginary and the frequency ω can be shown to be real (no damping in time) when $\epsilon_a = 0$ or $\max(\epsilon_i,\ \epsilon_a) \leq \sqrt{2}$. The proof of these properties is detailed in Appendix A.1. It is important to note that ω is forced to be real by the boundary dispersion relation, and that other solutions are possible when considering the inner dispersion relation only. These solutions will not be discussed in the following, even in Section 3 on waves in an unbounded ocean.

This means that in physically realistic conditions (i.e. $\max(\epsilon_i,\ \epsilon_a) \leq \sqrt{2}$) waves are either propagating or evanescent (but not both) along the vertical axis and that they are stable in time: real-δ_z waves are *propagating vertically* while imaginary-δ_z waves are *evanescent vertically*. Imaginary vertical wave-numbers will be written:

$$\delta_z = i\delta_{z,i} \quad \text{with} \quad \delta_{z,i} \in \mathbb{R} \tag{39}$$

The inner and boundary dispersion relations (35a) and (35b) write in this case:

$$\delta_x^2 - \delta_{z,i}^2 = \epsilon_i^2 \frac{\delta_x^2}{\omega^2} + \epsilon_a^2\omega^2 - \epsilon^4 \tag{40a}$$

$$\omega^2 = \frac{\delta_x^2 \tanh(\delta_{z,i})}{\delta_{z,i} + \epsilon^2 \tanh(\delta_{z,i})} \tag{40b}$$

When not explicitly mentioned, the standard values of the parameters used in the rest of the paper are listed in Table 2. The rest of the paper is organized as follows: the inner dispersion relation corresponding to waves in an unbounded ocean is studied in Section 3. Additional constraints related to the boundary dispersion relation, i.e., in a bounded ocean, are added in Section 4.

3. Inner dispersion relation & waves in an unbounded ocean

The inner dispersion relation (35a) must be satisfied by any type of ocean waves whether or not the ocean is considered as a locally unbounded medium (far from surface and bottom and for wavelengths small compared to ocean depth). We will show in the present section that (i) in $(\delta_x,\ \delta_z,\ \omega)$ phase-space, the inner dispersion relation leads to a dispersion surface that can be decomposed in three distinct regions corresponding to acoustic, surface and internal waves, (ii) two acoustic and stratification reference functions $\omega_a(\delta_x,\ \delta_z)$ and $\omega_i(\delta_x,\ \delta_z)$ are good approximations of the acoustic and internal regions which in turn correspond to acoustic and internal waves propagating in an unbounded ocean, (iii) the upper and lower regions of the inner dispersion surface (for respectively high and low frequencies) correspond to acoustic waves and internal waves propagating in an unbounded ocean and (iv) the bounded central region of the inner dispersion surface corresponds to vertically vanishing waves, which are referred to as surface waves in Section 4.

Table 2
Main parameters used to plot dispersion relations.

Gravity	g	9.8 m s^{-2}
Sound speed	c_s	1500 m s^{-1}
Depth	H	4000 m
Brunt-V$^{\grave{}}$ais$^{\acute{}}$älä frequency	$N = \sqrt{-\frac{g}{\bar{\rho}_h(z)}\frac{\partial\bar{\rho}_h}{\partial z} - \frac{g^2}{c_s^2}}$	10^{-3} s^{-1}
Acoustic small parameter	$\epsilon_a = \frac{\sqrt{gH}}{c_s}$	≈ 0.132
Internal small parameter	$\epsilon_i = \sqrt{\frac{N^2H}{g}}$	≈ 0.02020
Equivalent-stratification small parameter	$\epsilon = \sqrt{\frac{\epsilon_i^2+\epsilon_a^2}{2}}$	$\approx 9.44\text{x}10^{-2}$
Depth scale	$D_0 = \frac{H}{2\epsilon^2}$	≈ 224 km

3.1. Acoustic and stratification reference frequencies

Reference acoustic & stratification functions. Following Tolstoy (1963), the inner dispersion relation (35a) can be reformulated in the simpler form:

$$\frac{\omega^2}{\omega_a^2} + \frac{\omega_i^2}{\omega^2} = 1 \tag{41}$$

where ω_i and ω_a are functions of horizontal and vertical wave-numbers, defined by:

$$\omega_a^2(\delta_x,\ \delta_z) = \frac{1}{\epsilon_a^2}\left(\delta_x^2 + \delta_z^2 + \epsilon^4\right) \tag{42a}$$

$$\omega_i^2(\delta_x,\ \delta_z) = \frac{\delta_x^2\ \epsilon_i^2}{\delta_x^2 + \delta_z^2 + \epsilon^4} \tag{42b}$$

These two reference functions are not roots of the inner dispersion equation (41) but they are useful in their approximation and, more specifically, in their physical interpretation:

- If $\epsilon_a^2\omega^2 \gg \frac{\epsilon_i^2\delta_x^2}{\omega^2}$ (high frequency) then (41) simplifies to $\omega^2 \approx \omega_a^2$, relevant to a compressible, homogeneous (unstratified) ocean.
- If $\epsilon_a^2\omega^2 \ll \frac{\epsilon_i^2\delta_x^2}{\omega^2}$ (low frequency) then (41) simplifies to $\omega^2 \approx \omega_i^2$, relevant to an incompressible, stratified ocean.

Therefore ω_a can be interpreted as a *reference acoustic function* accounting for the compressibility content of the inner dispersion relation, and is a solution of the *inner* dispersion relation for an homogeneous ocean. ω_i plays an equivalent role for ocean stratification: it can be interpreted as a *reference stratification function* and is solution of the *inner* dispersion relation for an incompressible ocean.

Recall that for $\epsilon_a = 0$ or $max(\epsilon_i, \epsilon_a) \leq \sqrt{2}$ the frequency ω is real and δz is either real or purely imaginary (Appendix A.1). In addition, ω_a^2 and ω_i^2 have the same sign, since their product is equal to $\delta_x^2\frac{\epsilon_i^2}{\epsilon_a^2} > 0$. Therefore (41) implies that $\omega_a^2 \geq 0,\ \omega_i^2 \geq 0$, and that:

$$0 \leq \omega_i^2(\delta_x, \delta_z) \leq \omega^2(\delta_x, \delta_z) \leq \omega_a^2(\delta_x, \delta_z) \qquad \forall(\delta_x, \delta_z)$$

As a consequence, the frequency ω is always bounded by the reference functions ω_i and ω_a.

3.2. Roots of the inner dispersion relation ($\omega_\pm$)

Let us now define $R(\delta_x, \delta_z)$ the ratio of stratification to acoustic reference functions:

$$R^2(\delta_x, \delta_z) = \frac{\omega_i^2}{\omega_a^2} = \frac{\epsilon_a^2\epsilon_i^2\delta_x^2}{\left(\delta_x^2 + \delta_z^2 + \epsilon^4\right)^2} \tag{43}$$

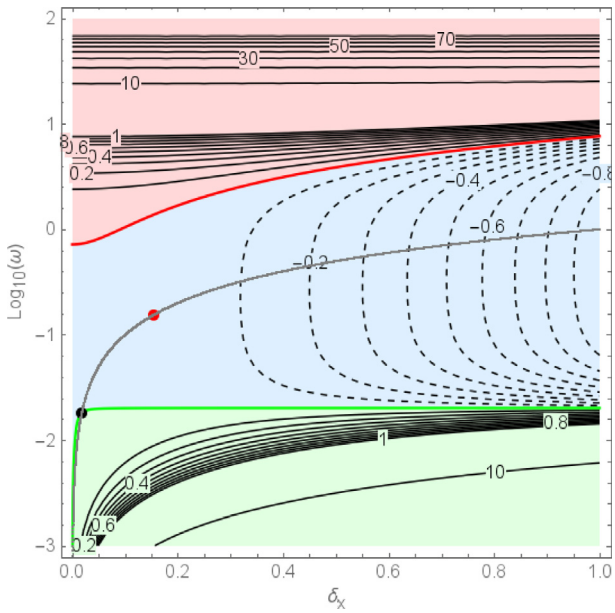

Fig. 1. Contours of $\delta_z^2(\delta_x,\ \omega)$. Plain lines represent positive values ($\delta_z \in \mathbb{R}$), and dashed lines negative values ($\delta_z \in i\mathbb{R}$). Background color: (light red) Modified Acoustic Waves -MAW-, (light blue) Modified Surface Waves -MSW-, light (green) Modified Internal Waves -MIW-. Black point: barotropic wave solution Section 2.6. Red Point: marginally stable MSW Section 4.5. Red and green curves: acoustic and gravity transition lines Section 3.3. For the values of the parameters listed in Table 2, $\delta_x = 1$ corresponds to a wave-number $k_x = 1/H = 1/4000$ m^{-1} and $log_{10}(\omega) = 0$ to a frequency $\Omega \approx 20$ s^{-1}. See text below for the definition of the different types of waves.

$R(\delta_x,\ \delta_z)$ is an important parameter for locating the roots of the inner dispersion relation. As shown in Appendix A.1, ω, the roots of Eq. (41), can only be real, a consequence is that $R^2 \le \frac{1}{4}$. These roots can then be formulated for the squared frequency:

$$\omega_\pm^2 = \frac{\omega_a^2}{2}\left(1 \pm \sqrt{1 - 4\frac{\omega_i^2}{\omega_a^2}}\right) = \frac{\omega_a^2}{2}\left(1 \pm \sqrt{1-4R^2}\right) \tag{44}$$

When R^2 is small, the two roots are close to the acoustic and stratification reference functions: $\omega_+ \approx \omega_a,\ \omega_- \approx \omega_i$. Since their product $\omega_-^2\omega_+^2$ is always equal to $\omega_a^2\omega_i^2 = \frac{\epsilon_i^2}{\epsilon_a^2}\delta_x^2$, we further have:

$$0 \le \omega_i^2(\delta_x,\delta_z) \le \omega_-^2(\delta_x,\delta_z) \le \frac{\epsilon_i}{\epsilon_a}\delta_x \le \omega_+^2(\delta_x,\delta_z) \le \omega_a^2(\delta_x,\delta_z). \tag{45}$$

Note also that for a weakly compressible ocean ($\epsilon_a \ll 1$):

$$\omega_-^2 - \omega_i^2 = -\frac{256\ \epsilon_a^4\epsilon_i^6\delta_x^2}{(\delta_x^2+\delta_z^2+\epsilon_i^4)^5} + O(\epsilon_i^6), \tag{46}$$

and for a weakly stratified ocean ($\epsilon_i \ll 1$ *and* $\epsilon \ll 1$):

$$\omega_+^2 - \omega_a^2 = \frac{\epsilon_a^2\epsilon_i^4}{(\delta_x^2+\delta_z^2+\epsilon_a^4/4)^3} + O(\epsilon_a^6) \tag{47}$$

3.3. Three regions in $(\delta_x,\ \delta_z,\ \omega)$ phase-space

Fig. 1 shows variations of the squared vertical wave-number δ_z^2 as a function of $(\delta_x,\ \omega)$ for the values of ϵ_i, ϵ_a given in Table 2. Negative values are encountered for medium-range frequencies ($10^{-1.7} < \omega < 10^{0.7}$) and large enough horizontal wave-numbers ($\delta_x \ge 0.1 - 0.2$). This region is surrounded by high and low frequency regions of positive δ_z^2. The transition lines between these regions are given by $\delta_z = 0$:

- If $\omega \gg 1$ and $\epsilon_a \ne 0$ then $\omega^2 \approx \omega_a^2$ and the acoustic transition line is given by $\epsilon_a^2\omega^2 \approx \delta_x^2 + \epsilon^4$. This line is a parabola and the frequency is not bounded when δ_x increases.
- If $\omega \ll 1$ and $\epsilon_i \ne 0$ then $\omega^2 \approx \omega_i^2$, the equation of the gravity transition line is $\omega^2 \approx \delta_x^2\epsilon_i^2/(\delta_x^2+\epsilon^4)$. This line has an upper bound $\omega_{c,i} = \epsilon_i$. This parabola crosses the $\delta_x = 0$-axis for the acoustic cut-off frequency $\omega_{c,a} = \epsilon^2/\epsilon_a$. In dimensional form, this bound can be rewritten $\Omega \le N$ and is related to the well-known cut-off frequency for internal gravity waves.

For a real frequency ω, Fig. 1 confirms that the vertical wave-number can only be real or imaginary and that the inner dispersion relation (35a) authorizes three types of wave solutions: two with real vertical wave-numbers ($\delta_z^2 \ge 0$) and one with purely imaginary wave-numbers ($\delta_z^2 < 0$). In this latest region, the corresponding wave solution is evanescent.

Separation of solutions. We prove in Appendix A.2 that, for a non-trivial (non-vanishing) wave solution in a stratified ocean, $R^2(\delta_x,\delta_z)$ can be equal to 1/4 only if δ_z is imaginary. In this case, $R^2(\delta_x,\delta_z) = 1/4$ leads to (A.19) and (A.20):

$$\delta_z^2 = -\delta_{z,i,*}^2 = -\delta_x^2 - \epsilon^4 + 2\epsilon_a\epsilon_i\delta_x \tag{48a}$$

$$\omega^2 = \omega_-^2 = \omega_+^2 = \frac{\epsilon_i}{\epsilon_a}\delta_x = \frac{\omega_a^2}{2} \tag{48b}$$

A consequence is that wave solutions are well-separated when δ_z is real (and does not vanish) or when δ_z is imaginary and $\delta_{z,i} < \delta_{z,i,*}$. Even if (40a) has two roots in this case, the two corresponding branches are always connected for $(\delta_z^2,\ \omega^2)$ satisfying (48a)–(48b), and thus form a single family of ocean waves.

3.4. Wave solutions in an unbounded ocean

For a real vertical wave-number ($\delta_z \in \mathbb{R}$),[2] the two roots are thus always well-separated and given by:

$$\omega_-(\delta_x,\ \delta_z) \approx \omega_i(\delta_x,\ \delta_z), \quad \omega_+(\delta_x,\ \delta_z) \approx \omega_a(\delta_x,\ \delta_z) \tag{49}$$

Modified internal waves (MIW). The traditional dispersion relation for dispersive internal gravity waves in the context of a Boussinesq incompressible fluid (Gill 1982; see also Table 1 above) is:

$$\omega^2 = \omega_{igr}^2 = \epsilon_i^2\frac{\delta_x^2}{\delta_x^2+\delta_z^2} \tag{50}$$

A Taylor expansion of the gravity-wave root ω_-^2 given by (44) with respect to the small parameters ϵ_a and ϵ_i leads to:

$$\frac{\omega_-^2}{\omega_{igr}^2} = 1 - \left(\frac{\epsilon^4}{\delta_x^2+\delta_z^2} - \frac{\epsilon_i^2\epsilon_a^2\delta_x^2}{(\delta_x^2+\delta_z^2)^2}\right) + O(\epsilon^8) \tag{51}$$

$$= 1 - \underbrace{\frac{\epsilon^4\delta_z^2 + 4(\epsilon_a^2-\epsilon_i^2)^2\delta_x^2}{(\delta_x^2+\delta_z^2)^2}}_{O(\epsilon^4)} + O(\epsilon^8), \tag{52}$$

while the development of ω_i^2 leads to

$$\frac{\omega_i^2}{\omega_{igr}^2} = 1 - \underbrace{\frac{\epsilon^4}{\delta_x^2+\delta_z^2}}_{O(\epsilon^4)} + O(\epsilon^8).$$

Compared with ω_i^2, ω_-^2 includes corrective terms confirming that the two roots of the inner dispersion relation are not fully separated. The corrective term $\frac{\epsilon_i^2\epsilon_a^2\delta_x^2}{4(\delta_x^2+\delta_z^2)^2}$ is naturally close to R^2. Formulation (52) shows that the combined effect of compressibility and stratification is always a reduction of the frequency, compared with the approximated value ω_{igr}: $\omega_-^2 \le \omega_{igr}^2$.

Ocean waves satisfying (51) will now be referred to as *Modified Internal Waves (MIW)*.

[2] Imaginary vertical wave-numbers ($\delta_z \in i\mathbb{R}$) are treated in Section 4.4 for a bounded ocean.

Modified acoustic waves (MAW). The well-known dispersion relation for acoustic waves in an homogeneous fluid is (Table 1):

$$\omega_{aw}^2 = \frac{1}{\epsilon_a^2}\left(\delta_x^2 + \delta_z^2\right) \tag{53}$$

A Taylor development of the acoustic root (ω_+) with respect to ϵ_a and ϵ_i leads this time to:

$$\frac{\omega_+^2}{\omega_{aw}^2} = 1 + \left(\frac{\epsilon^4}{2(\delta_x^2+\delta_z^2)} - \frac{\epsilon_i^2\epsilon_a^2\delta_x^2}{(\delta_x^2+\delta_z^2)^2}\right) + \mathrm{O}(\epsilon^8) \tag{54}$$

$$= 1 + \underbrace{\frac{\epsilon^4\delta_z^2 + (\epsilon_a^2-\epsilon_i^2)^2\delta_x^2}{2(\delta_x^2+\delta_z^2)^2}}_{\mathrm{O}(\epsilon^4)} + \mathrm{O}(\epsilon^8), \tag{55}$$

while the development of ω_a^2 leads to

$$\frac{\omega_a^2}{\omega_{aw}^2} = 1 + \underbrace{\frac{\epsilon^4}{\delta_x^2+\delta_z^2}}_{\mathrm{O}(\epsilon^4)} + \mathrm{O}(\epsilon^8).$$

Compared with ω_a^2, ω_+^2 includes corrective terms due to the two roots of the inner dispersion relation not being fully separated. Again, the corrective term is small and close to R^2. The combined effect of compressibility and stratification is always an increase of the frequency, compared with the approximated value ω_{aw}: $\omega_+^2 \geq \omega_{aw}^2$.

Ocean waves satisfying (54) will be called *Modified Acoustic Waves (MAW)* in the following. The modifications to usual internal and acoustic wave dispersion relations by compressibility and stratification effects are expressed by:

$$\omega_+^2\omega_-^2 = \frac{\epsilon_i^2}{\epsilon_a^2}\delta_x^2 = \omega_{aw}^2\omega_{igr}^2,$$

which can explain the symmetry in the above developments for modified internal and acoustic waves.

3.5. Homogeneous and/or incompressible unbounded ocean

Much insight can be gained on acoustic-gravity waves by a geometrical investigation of surfaces (in phase space) that correspond to the inner and boundary dispersion relations. These surfaces will respectively be named *inner and boundary dispersion surfaces*.

Fig. 2 shows the inner dispersion surfaces in the (δ_x, δ_z, ω) space. Each dispersion surface corresponds to a region of the wave solutions. These surfaces are plotted for a homogeneous and incompressible (2.a), a homogeneous and compressible (2.b), an incompressible and stratified (2.c) and a compressible and stratified unbounded ocean. The y-axis is constructed such that the ($\delta_z > 0$) positive half-space corresponds to the real vertical wave-numbers whereas the ($\delta_z < 0$) negative half-space corresponds to the (imaginary part of) pure-imaginary vertical wave-numbers ($\delta_{z,i}$).

Careful inspection of the ($\delta_z > 0$) half space in Figs. (2.b), (2.c) and (2.d) confirms the presence of two regions of solutions with real positive vertical wave-numbers. For large frequencies (red branch), the upper region corresponds to acoustic wave solutions (MAW) (Figs. 2.b and 2.d). This region disappears under the assumption of incompressibility (Figs. 2.a and 2.c). The lower region (light-green branch) corresponds to internal wave solutions (MIW) (Figs. 2.c and 2.d) and disappears under the assumption of homogeneous ocean (Figs. 2.a and 2.b).

The third region of wave-solution (light-blue surfaces in Fig. 2) corresponds to pure-imaginary vertical wave-numbers. In a stratified, compressible, unbounded ocean (Fig. 2.d), this region corresponds to intermediate values of the .

In a homogeneous, incompressible and unbounded ocean, Fig. 2.(a) shows that the unique dispersion surface is the ($\delta_x^2 = -\delta_z^2$) plane.

3.6. Summary: waves solutions in an unbounded ocean

In the preceding analysis, three types of waves were identified. A synthesis is given by Fig. 2.d showing the inner dispersion surfaces for a stratified, compressible ocean and Fig. 2.a–c showing the limit cases for respectively a homogeneous and incompressible, a homogeneous and compressible and a stratified but incompressible ocean. Approximate frequency values for modified internal and acoustic waves are summarized in Tables 3 and 4 in dimensional form, for comparison with introductory Table 1. Since the practical existence and characterization of modified surface waves is totally dependent on boundary conditions, they are not summarized here but will be detailed in the next section.

In a more realistic bounded ocean, their existence is guaranteed only if their vertical scale is (much) smaller than the ocean depth ($|\delta_z| \gg 1$) and if they do not interfere with the bottom or the surface of the ocean. The next section will investigate the impact of adding the boundary dispersion relation (35b).

4. Waves in a bounded ocean

Acoustic-gravity waves propagating in a bounded ocean (i.e. considering both the free-surface and the bottom boundary of the ocean) are studied in the present section. These wave solutions are first shown to be organised in branches (i.e. in 1D curves parameterized by ($\delta_x^2(\delta_z)$, $\omega^2(\delta_z)$). Each branch is located at the intersection of the inner and boundary dispersion surfaces and is confined to a region of phase space located between two poles of the dispersion relations.

Modified internal and acoustic modes and then modified surface waves are studied before acoustic-gravity waves in the long wave approximation are investigated.

4.1. Graphical investigation of Modified Surface Waves (MSW), Modified Acoustic Modes (MAM) and Modified Internal Modes (MIM)

The compressible and stratified ocean is now assumed to be bounded. Wave solutions must thus satisfy both the inner (35a) and boundary (35b) dispersion relations. In phase space, they must lie at the intersections of the inner and boundary dispersion surfaces, which are now plotted simultaneously on Fig. 3. For real vertical wave-numbers ($k_z \in \mathbb{R}$, Fig. 3a), the boundary dispersion surface is a piecewise surface. Several regions that are nearly vertical in (δ_x, δ_z, $\log_{10}(\omega)$) space at $\delta_z \approx n\pi$ (small ω) and at $\delta_z \approx \pi/2 + (m-1)\pi$ (large ω) with $n \in \mathbb{N}^*$ and $m \in \mathbb{N}^*$. The intersection of these surfaces with inner dispersion relation surfaces result in a number of constrained vertical wave-numbers (according to n and m). We will show in the following sections that the resulting wave solutions are "modes" and the two intersections correspond more specifically to *Modified Internal Modes (MIM)*, $n \in \mathbb{N}^*$ and to *Modified Acoustic Modes (MAM)*, $m \in \mathbb{N}^*$.

For purely imaginary wave-numbers, the (light blue) inner dispersion surface looks like an horizontal hyperbolic surface which intersects the (light gray) boundary dispersion surface. The resulting wave solutions correspond to *Modified Surface Waves (MSW)*. Far from the origin $(\delta_x, \delta_z) = (0,0)$, at the intersection points, $|\delta_z|$ is close to δ_x.

For long waves ($\delta_x \ll 1$ & $|\delta_z| \ll 1$), the boundary dispersion surfaces for real and purely imaginary δ_z are in the same plane. Indeed, the development of the boundary relation is well approximated by $\omega^2 \approx \delta_x^2$ in both cases (a better approximation is given in Eq. (67)). Fig. 3b shows the different solutions close to the origin $(\delta_x, \delta_z, \omega) = (0,0,0)$. The acoustic-wave surface does not intersect the boundary dispersion surface near the origin (as proven in Section 4.5) and is not present close to the origin.

In the context of a bounded ocean, three types of wave solutions are thus graphically identified, spreading on the three regions of the inner dispersion surface, while satisfying the boundary dispersion relation: internal gravity (in a stratified ocean), acoustic (in a compressible

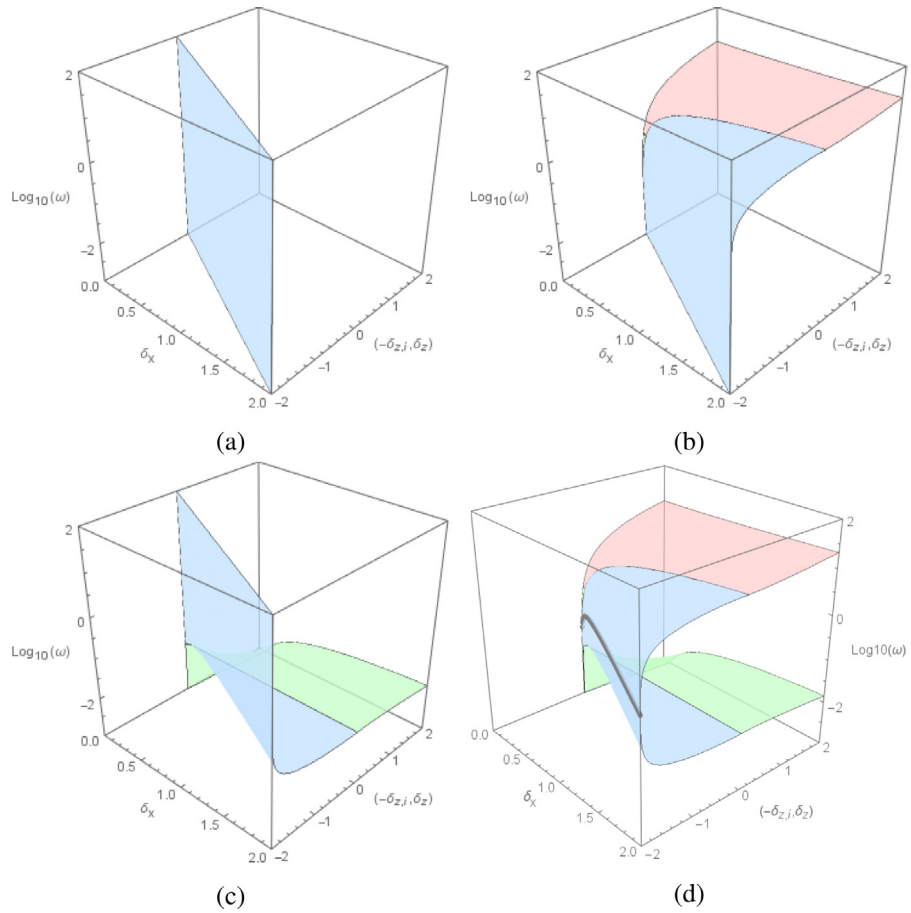

Fig. 2. Inner dispersion surfaces in (δ_x, δ_z, ω) space.
(a) homogeneous, incompressible ocean ($\epsilon_i = \epsilon_a = 0$),
(b) homogeneous, compressible ocean ($\epsilon_i = 0$),
(c) stratified, incompressible ocean ($\epsilon_i = 0$),
(d) stratified, compressible ocean ($\epsilon_a = 0$).
Colors: (light red) acoustic wave region ($\delta_z^2 \geq 0 \& \omega$ large), (light blue) surface wave region ($\delta_z^2 \geq 0 \& \omega$ small), (light green) internal wave region ($\delta_z^2 < 0$). Gray curve: triplets ($\delta_x, \delta_z, \omega$) satisfying (48b) and (48a). Negative values of the δ_z axis correspond to $-\delta_{z,i}$, i.e. minus the imaginary part of imaginary vertical wave-numbers. For the values of the parameters listed in Table 2, $\delta_x = 1$ ($\delta_z = 1$) corresponds to a wave-number $k_x = 1/H = 1/4000$ m^{-1} ($k_z = 1/H = 1/4000$ m^{-1}) and $log_{10}(\omega) = 0$ to a frequency $\Omega \approx 20$ s^{-1}.

Table 3
Modified Internal and Acoustic waves in an unbounded ocean.

	Internal Waves	Acoustic Waves
(a) ($\epsilon_i = \epsilon_a = 0$)	–	–
(b) ($\epsilon_i = 0, \epsilon_a \neq 0$)	–	$\frac{\omega_+^2}{\omega_{aw}^2} \approx 1 + \frac{\epsilon_a^4}{4(\delta_x^2 + \delta_z^2)}$
(c) ($\epsilon_i \neq 0, \epsilon_a = 0$)	$\frac{\omega_-^2}{\omega_{iwr}^2} \approx 1 - \frac{\epsilon_i^4}{4(\delta_x^2 + \delta_z^2)}$	–
(d) ($\epsilon_i \neq 0, \epsilon_a \neq 0$)	$\frac{\omega_-^2}{\omega_{iwr}^2} \approx 1 - \frac{(\epsilon_i^2 + \epsilon_a^2)^2 \delta_z^2 + (\epsilon_a^2 - \epsilon_i^2)^2 \delta_x^2}{4(\delta_x^2 + \delta_z^2)^2}$	$\frac{\omega_+^2}{\omega_{aw}^2} \approx 1 + \frac{(\epsilon_i^2 + \epsilon_a^2)^2 \delta_z^2 + (\epsilon_a^2 - \epsilon_i^2)^2 \delta_x^2}{4(\delta_x^2 + \delta_z^2)^2}$

Table 4
Compressibility and stratification induced modifications to the usual dispersion relations given in table Table 1. Ω is wave frequency, k_x and k_z are the wavenumbers, g is the acceleration of gravity, N a reference Brunt-V̀aisf́alä frequency and c_s the speed of sound. D_0 is the background density vertical scale, given by $1/D_0 = N^2/g + g/c_s^2$. The orders of magnitude of the modifications (last column) are computed for the values of the main parameters given in table Table 2 and $k_x = k_z = 1/H$.

Waves	Frequency (Ω)	Modification (%)
Modified Acoustic Waves (MAW)	$\Omega_{maw}^2 = c_s^2(k_x^2 + k_z^2)\left[1 + \frac{1}{4(k_x^2 + k_z^2)^2}\left(\frac{k_z^2}{D_0^2} + \left(\frac{g}{c_s^2} - \frac{N^2}{g}\right)^2 k_x^2\right)\right]$	3.8x10^{-3}
Modified Internal Waves (MIW)	$\Omega_{miw}^2 = \frac{N^2 k_x^2}{k_x^2 + k_z^2}\left[1 - \frac{1}{4(k_x^2 + k_z^2)^2}\left(\frac{k_z^2}{D_0^2} + \left(\frac{g}{c_s^2} - \frac{N^2}{g}\right)^2 k_x^2\right)\right]$	−3.8x10^{-3}

ocean) and surface waves (in a free-surface ocean). They are investigated in the following using Taylor expansions of the general roots $\omega_\pm$, with respect to small parameters (ϵ_i, ϵ_a), leading to simple approximations of wave dispersion relations. When needed, asymptotic relations

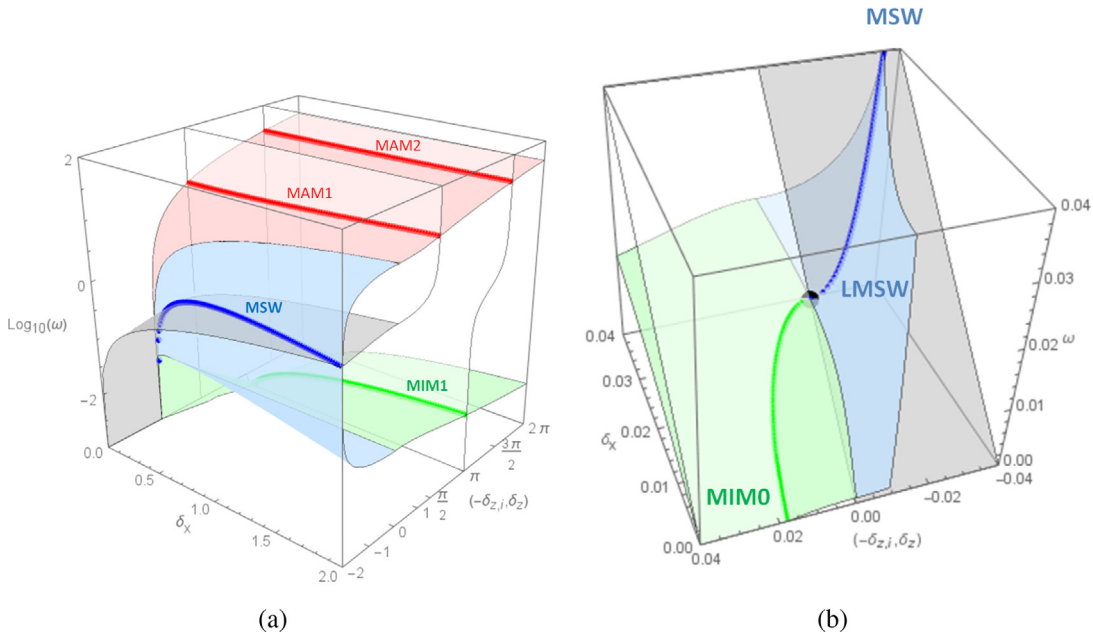

Fig. 3. Inner and boundary dispersion surfaces in $(\delta_x,\ \delta_z, \omega)$ space and wave solutions for short and intermediate wavelengths (a) and for long waves (b). Colors: (light red) acoustic wave region ($\delta_z^2 \geq 0 \& \omega$ large), (light blue) surface wave region ($\delta_z^2 \geq 0 \& \omega$ small), (light green) internal wave region ($\delta_z^2 < 0$), (white) boundary dispersion surface for $\delta_z \in \mathbb{R}$, (light gray) boundary dispersion surface for $\delta_z \in \mathbb{R}$. Blue curve: Modified Surface Waves (MSW). Red curves: Modified Acoustic Modes (MAM). Green curve: Modified Internal Modes (MIM). Black point: depth-independent surface gravity wave Section 2.6.

are derived with respect to δ_x, δ_z or ω. Taylor expansions will give indications of how usual wave solutions can be modified by gravity and stratification (ϵ_i), and/or by compressibility (ϵ_a).

4.2. Poles of the dispersion relations

The dispersion relations for acoustic-gravity waves in a bounded ocean exhibit several discrete poles or singularities (for the vertical wave-number) that lead to the existence of normal modes. To show this, we can combine the dispersion relations (35a) and (35b) to express the square of the horizontal wave-number and the frequency as functions of the vertical wave number:

$$\delta_x^2(\delta_z) = \frac{\left(\epsilon^2 \sin(\delta_z) + \delta_z \cos(\delta_z)\right)\left((\delta_z^2 + (\epsilon_i^4 - \epsilon_i^4)/4)\sin(\delta_z) - \delta_z \epsilon_i^2 \cos(\delta_z)\right)}{\left((\epsilon_a^2 - \epsilon_i^2)\sin(\delta_z)/2 - \delta_z \cos(\delta_z)\right)\sin(\delta_z)} \tag{56a}$$

$$\omega_x^2(\delta_z) = \frac{(\delta_z^2 + (\epsilon_a^4 - \epsilon_i^4)/4)\sin(\delta_z) - \delta_z \epsilon_i^2 \cos(\delta_z)}{(\epsilon_a^2 - \epsilon_i^2)\sin(\delta_z)/2 - \delta_z \cos(\delta_z)} \tag{56b}$$

The first relation (56a) has two poles (or singularities): $\delta_z = \delta_{z,n} = n\pi$ with $n \in \mathbb{N}$ is indeed an approximate root of $\sin(\delta_z) = 0$ and thus a pole of $\delta_x^2(\delta_z)$ and $\delta_z = \delta_{z,m} \approx r_m = \pi/2 + m\pi$ is a root of $\delta_z/\tan(\delta_z) = \epsilon_a^2 - \epsilon_i^2 \ll 1$ and thus a pole of $\delta_x^2(\delta_z)$. The second dispersion relation (56b) only has one pole: $\delta_z = \delta_{z,m} \approx r_m = \pi/2 + m\pi$. A more accurate expression of $\delta_{z,m}$ can be obtained as an infinite series:

$$\delta_{z,m} = r_m - \frac{\epsilon_a^2 - \epsilon_i^2}{r_m} - \frac{(\epsilon_a^2 - \epsilon_i^2)^2(3 + \epsilon_i^2 - \epsilon_a^2)}{3r_m^3} - \frac{(\epsilon_a^2 - \epsilon_i^2)^3\left(3(\epsilon_a^2 - \epsilon_i^2)^2 - 20(\epsilon_a^2 - \epsilon_i^2) + 30\right)}{15 r_m^5} + O(\frac{1}{r_m^7}) \tag{57}$$

Note that $\omega^2(\delta_z)$ is continuous in $\delta_z = \delta_{z,n}$. This set of poles confirms and extends the poles found by Jensen et al. (2011) for a compressible, homogeneous, rigid lid, "ideal ocean waveguide".

These poles are associated to the AG modes discussed in Section 2. To show this, one can follow Jensen et al. (2011) and rewrite the wave field emitted by a point source at frequency ω alternatively as a line integral or as an infinite series in Fourier space. The poles are then the singularities of the line integral whereas the series is the infinite sum of discrete modes. The equivalence of both expressions is given by Cauchy's residue theorem (Mei et al., 2005).

We further show in A.3 that the first type ($\delta_{z,m}$) corresponds to the Modified Acoustic Modes (MAM) identified graphically in Section 4.1 and plotted with a red curve in Fig. 3. The second type ($\delta_{z,n}$) is also shown to correspond to the Modified Internal Modes (MIM) also identified graphically in Section 4.1 but plotted in green.

Fig. 4 shows that wave solutions are organized in branches confined to the intervals $\delta_z^2 \in (-\infty, \delta_{z,m=1}^2)$, $\delta_z \in (\delta_{z,m=n}, \delta_{z,n})$ and $\delta_z \in (\delta_{z,n}, \delta_{z,m=n+1})$ for $n \in \mathbb{N}^*$. The $\delta_x^2 + \delta_z^2 = 0$ vertical plane, coloured in light gray, is the region where the induced effects of compressibility and stratification exactly compensate. Indeed, (35a) implies in this case that $\epsilon_a^2\omega^2 + \epsilon_i^2\delta_x^2/\omega^2 - \epsilon = 0$.

A study of the variations of $\delta_x^2(\delta_z)$ and $\omega^2(\delta_z)$ shows that these functions are monotonically decreasing at respectively the third and first order in (ϵ_a, ϵ_i) (see Appendix A.7). When $\delta_z \to \delta_{z,m}^{\pm}$, $\delta_x^2(\delta_z) \to \pm\infty$ and $\omega^2(\delta_z) \to \pm\infty$. When $\delta_z \to \delta_{z,n}^{\pm}$, $\delta_x^2(\delta_z) \to \pm\infty$ but $\omega^2(\delta_z) = \pm\epsilon_i^2$ since $\delta_{z,n}$ is not a pole of $\omega(\delta_z)$. In the interval $(-\infty, \delta_{z,m=0}]$, the long-wave branch extends to negative values of δ_z^2 (for an imaginary vertical wave-number, blue curve in Fig. 4. Each branch of the acoustic gravity wave solutions consequently extends both in the $\delta_x^2 \geq 0$ half space of propagating waves (green, red and blue curves in Fig. 4) and in the $\delta_x^2 < 0$ half space of vanishing waves (gray and black curves).

This study of the variations of $\delta_x^2(\delta_z)$ further shows that for waves propagating both horizontally and vertically ($\delta_x^2,\ \delta_z^2 \geq 0$), δ_z remains close to either $\delta_{z,m}$ or $\delta_{z,n}$ in each interval of solutions except for the very-long-wave branch (Fig. 4.c and $0 < \delta_z^2 < \delta_{z,m=0} \approx \pi/2$). Indeed, in the case of "not-too-long" propagating waves, $\delta_x^2 + \delta_z^2$ is positive and at least larger than $\delta_{z,m=0}^2$ meaning that, whatever δ_x, either $\epsilon_a^2\omega^2 = \epsilon_a^2\delta_x^2/\left(\epsilon^2 + \delta_z \operatorname{cotan}(\delta_z)\right)$ or $\epsilon_i^2\delta_x^2/\omega^2 = \epsilon_i^2\left(\epsilon^2 + \delta_z \operatorname{cotan}(\delta_z)\right)$ are significantly large. This is possible only if respectively $\delta_z \approx \delta_{z,m}$ (Section 4.3.2) or $\delta_z \approx \delta_{z,n}$ (Section 4.3.1). Graphically, Fig. 4.a, b and d confirm that δ_z varies sharply only in regions where $\delta_x^2 + \delta_z^2 \approx 0$ i.e. in regions where the acoustic gravity wave solutions are close to the (gray) vertical surface ($\delta_x^2 + \delta_z^2 = 0$).

The study of the poles finally confirms the separation of the branches of the acoustic gravity wave solutions in agreement with the

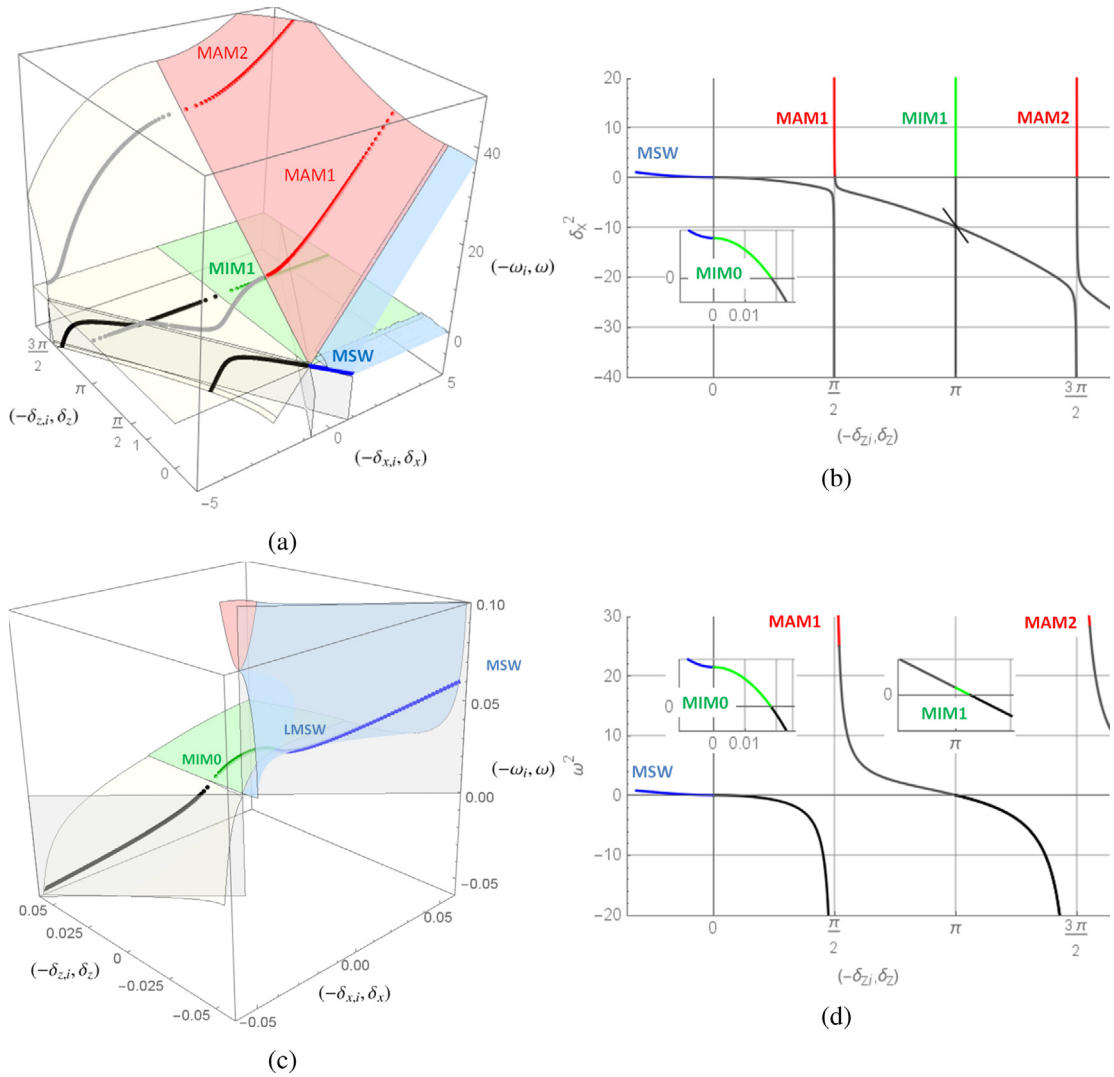

Fig. 4. (a, c) show the inner and boundary dispersion surfaces in $(\delta_x,\ \delta_z, \omega)$ space and wave solutions for long waves, (b, d) show $\delta_x^2(\delta_z)$ and $\omega^2(\delta_z)$. Coloured surfaces: (light red) acoustic wave region, (light blue) surface wave region, (light green) internal wave region, (light yellow) inner dispersion surface in half space $\delta_x^2 < 0$, (light gray) $\delta_x^2 + \delta_z^2 = 0$ vertical plane. Acoustic gravity wave branches: MIM-0 (green curve), LMSW (blue curve) branch, MIM (green curves), MAM (red curves prolonged in gray when $\delta_x^2 < 0$), MIM (green curves prolonged in black when $\delta_x^2 < 0$). Note that wave solutions with imaginary horizontal wave-numbers ($\delta_{x,i} \in i\mathbb{R}$) or imaginary frequencies ($\omega \in i\mathbb{R}$) are plotted to clearly identify wave branches. These solutions correspond to waves decaying respectively in the horizontal direction and in time and are not further discussed in the present study.

results proved in Appendix A.2. Firstly, a clear separation has now been brought to light in terms of their vertical wave-numbers since the branches are confined to the interval regions locates between the poles: $\delta_z \in (\delta_{z,m=n}, \delta_{z,n})$ and $\delta_z \in (\delta_{z,n}, \delta_{z,m=m+1})$ for $n \in \mathbb{N}^*$. Secondly, in so far as the not-too-long wave solutions satisfy either $\delta_z \approx \delta_{z,m}$ or $\delta_z \approx \delta_{z,n}$, the relation (56b) further confirms that the solutions are also well-separated in terms of their frequency. Indeed, we have shown that $\delta_x^2 > 0$ imposes in this case that δ_z is close to either $\delta_{z,m}$ or $\delta_{z,n}$. Since (i) $\delta_{z,m}$ is a pole of ω^2 and thus $\omega^2(\delta_z \approx \delta_{z,m}\ and\ \delta_{z,m} < \delta_z)$ is large and (ii) $\omega^2(\delta_z)$ monotonic decreasing and $\omega^2(\delta_{z,n}) = \epsilon_i^2$, we can conclude and confirm that $\omega^2(\delta_z \approx \delta_{z,m}) \gg \epsilon_i^2 \geq \omega^2(\delta_z \approx \delta_{z,n}\ and\ \delta_{z,n} < \delta_z)$.

4.3. Real δ_z: modified internal and acoustic waves

As shown in Section 3.3 and Section 4.2, upper (acoustic) and lower (gravity) regions of the inner dispersion surface for real δ_z are well-separated: Modified Acoustic Modes (MAM) and Modified Internal Modes (MIM) solutions can thus be studied independently. We additionally showed that as long as δ_z is not close to zero, the acoustic gravity wave solutions remain close to one of the poles. The case of long waves with $\delta_z \approx 0$ is discussed in Subsection Section 4.5.

4.3.1. Development of internal-gravity modes modified by compressibility (MIM)

Waves can propagate horizontally between the bottom and surface of the ocean as in a wave guide. Internal gravity modes are well-known such examples (Gill, 1982). In Section 4.1, graphical inspections of wave solutions confirmed that gravity waves with constrained vertical wave-numbers could be found at the intersection of inner and boundary dispersion surfaces.

We have also shown in Section 3.3 that the root of the inner dispersion relation corresponding to internal gravity waves is well-approximated by ω_i^2 (46) and in Section 4.2 and Appendix A.3 that δ_z remains close to $\delta_{z,n}$.

In order to refine the approximation and to parameterize this relation in terms of the horizontal wave-number, we equate the squared frequency given by the surface dispersion relation (35b) to ω_-^2, given by the inner dispersion relation (44). This forms a non-linear equation for δ_z whose solution can be approximated using two passes of a Newton algorithm starting from $\delta_z = \delta_{z,n}$. Finally a Taylor development in $\epsilon_i,\ \epsilon_a$ leads to:

$$\delta_z(\delta_x) = \delta_{z,mim}(\delta_x) = \delta_{z,n}\left(1 + \frac{\epsilon_i^2}{\delta_x^2 + \delta_{z,n}^2} + \frac{(\delta_x^2 - \delta_{z,n}^2)}{(\delta_x^2 + \delta_{z,n}^2)^3}\epsilon_i^4\right) + \mathrm{O}(\epsilon^6) \qquad (58)$$

A development for the frequency ω^2 can be obtained by injecting expression (58) of δ_z in the general expression (51) in the unbounded domain case. The usual dispersion relation given in Table 1 can be written in dimensional form:

$$\omega^2(\delta_x) = \omega^2_{igr}\Big|_{\delta_z=\delta_{z,n}}(\delta_x) = \epsilon_i^2 \frac{\delta_x^2}{\delta_x^2+\delta_{z,n}^2} \tag{59}$$

Considering only the first order correction to this relation, we can omit all terms of order 3 in ϵ^2 in (51) to get:

$$\omega^2(\delta_x) = \omega^2_{mim}(\delta_x) = \underbrace{\epsilon_i^2 \frac{\delta_x^2}{\delta_x^2+\delta_{z,n}^2}}_{\omega^2_{im}}\left(1-\frac{2\epsilon_i^2\delta_{z,n}^2}{(\delta_x^2+\delta_{z,n}^2)^2}\right) + \mathrm{O}(\epsilon^6) \tag{60}$$

Therefore, the main correction to the usual dispersion relation comes from the fact that δ_z is not exactly equal to (but remains close to) $\delta_{z,n} = n\pi$. MIM correspond to the green curve in (Fig. 3.a).

4.3.2. Development of acoustic modes modified by gravity (MAM)

To study modified acoustic modes at higher frequencies, we now use the fact that the root of the inner dispersion relation corresponding to acoustic waves is well-approximated by ω_a^2 (47) and that δ_z remains close to $\delta_{z,m}$ Section 4.2 and A.3.

Again, in order to get a more accurate expression of δ_z parameterize by the horizontal wave-number δ_x, we equate the (inversed) squared frequency given by the surface dispersion relation (35b) to the (inversed) ω_+^2, given by the inner dispersion relation (44), and perform the nonlinear equation's solution approximation followed by a Taylor development in ϵ_i, ϵ_a to obtain:

$$\delta_z(\delta_x) = \delta_{z,mam}(\delta_x) = \delta_{z,m} - \frac{(\delta_x^2-\delta_{z,m}^2)}{2\delta_{z,m}(\delta_x^2+\delta_{z,m}^2)}\epsilon_a^2 + \frac{\epsilon_i^2}{2\delta_{z,m}^2} \underbrace{- \frac{\delta_x^6(\epsilon_a^2-\epsilon_i^2)^2 + 3\delta_x^2(\epsilon_a^2-\epsilon_i^2)^2\delta_{z,m}^2 - 2\delta_x^2(5\epsilon_a^2-3\epsilon_i^2)\epsilon^2\delta_{z,m}^4 + 2\epsilon^4\delta_{z,m}^6}{4(\delta_x^2+\delta_{z,m}^2)^3\delta_{z,m}^3}}_{\mathrm{O}(\epsilon^4)} + \mathrm{O}(\epsilon^6) \tag{61}$$

An expansion for the frequency ω^2 can be obtained by injecting the expression (61) of δ_z in the general expression (54) in the unbounded domain case. The main departure from to the usual acoustic wave frequency, given in Table 1 in dimensional form, is given by the second-order development:

$$\omega^2(\delta_x) = \omega^2_{mam}(\delta_x) = \frac{1}{\epsilon_a^2}\left[\delta_x^2+\delta_{z,m}^2 - \frac{(\delta_x^2-\delta_{z,m}^2)}{(\delta_x^2+\delta_{z,m}^2)}\epsilon_a^2 + \epsilon_i^2\right] + \mathrm{O}(\epsilon^2) \tag{62}$$

Here, stratification has a first-order (in ϵ_i^2) contribution to the modification of the homogeneous case frequency. This first-order modification comes from the first-order modification on the vertical wave-number itself (61). However, it is clear that the associated impact is small since ϵ_i^2 is negligible compared with $\delta_{z,m}^2$ in (61) and (62), because $\delta_{z,m} \geq \pi/2$. A similar conclusion was drawn in (Smith, 2015). MAM correspond to the red curves in (3.a).

4.4. Purely imaginary δ_z: modified surface acoustic-gravity waves (MSW)

"Surface waves" generally refer to waves propagating horizontally as anomalies of the ocean free-surface (Gill, 1982). In the vertical direction, these surface wave anomalies are "evanescent", meaning that, with the notation chosen in the present study, the vertical wave-number δ_z is a purely imaginary complex number. A Modified Surface Wave (MSW) defined by its triplet $(\delta_x, \delta_z, \omega)$ must satisfy both the inner (40a) and boundary (40b) dispersion relations for $\delta_z = i\,\delta_{z,i}$.

Homogeneous & incompressible ocean. In an homogeneous and incompressible ocean ($\epsilon_i = \epsilon_a = 0$, Fig. 2), the inner dispersion relation (40a) implies $\delta_{z,i} = \delta_x$. This equality is often postulated in textbooks to reduce the number of variables. Vertical polarization relations are then functions of δ_x only (Gill, 1982) and, as a consequence, the only remaining dispersion relation is the boundary dispersion relation (40b) for purely imaginary vertical wave-number ($\delta_z = i\delta_x$), or its approximation $\omega^2 = \delta_x \tanh\delta_x$. In this case, $\delta_{z,i}$ is reduced to a vertical length-scale of energy decay with increasing distance from the surface; for very long waves ($\delta_x \gg 1$), the surface wave (LSW) is approximately depth-independent (Table 1).

Dispersion relation. In the more general case (non homogeneous and compressible ocean), we prove in Appendix A.4 the existence of solutions to ((40a), (40b)). When the parameters ϵ_i and ϵ_a are small, we additionally prove in Appendix A.5 that surface acoustic-gravity waves have approximately similar horizontal and vertical wave-numbers ($\delta_x \approx \delta_{z,i}$).

This crude assumption $\delta_x \approx \delta_{z,i}$ is sufficiently accurate to recover usual swell-like approximations (Table 1), i.e., for sufficiently large δ_x (or δ_z). However a more accurate expression is given by:

$$\delta_{z,i}^2(\delta_x) = \delta_x^2 - \delta_x\left(\frac{\epsilon_i^2}{\tanh(\delta_x)} + \epsilon_a^2\tanh(\delta_x)\right) + \mathrm{O}(\epsilon^4). \tag{63}$$

In order to obtain (63), we introduce the frequency given by the boundary dispersion relation in the inner dispersion relation (40a) and solve the resulting nonlinear equation by performing one pass of a Newton algorithm. Note that the problem is formulated in terms of $\delta_{z,i}^2(\delta_x)$ since it can be shown (by looking at the error estimate of the Newton algorithm) that a formulation in terms of $\delta_{z,i}(\delta_x)$ is not accurate when δ_x is relatively small. Note also that (63) requires $\delta_x \geq \epsilon_i$ for $\delta_{z,i}^2$ to be positive. This is consistent with the fact that δ_x must be greater than $\delta_{x,0}(\approx \epsilon_i)$ defined in (38), as shown in Appendix A.4. However (63) does not allow us to recover the exact value $\delta_{x,0}$ of δ_x that cancels $\delta_{z,i}$, due to the first-order only approximation in terms of ϵ^2. The case of long surface waves with $\delta_{z,i}$ close to zero will be treated separately in Section 4.5.

The frequency $\omega^2(\delta_x)$ associated to the vertical wave-number $\delta_{z,i}^2(\delta_x)$ given by (63) is well approximated by:

$$\omega^2(\delta_x) = \delta_x\tanh(\delta_x)\left[1-\frac{1}{2}\left(\frac{\epsilon_i^2}{\sinh^2(\delta_x)} + \frac{\epsilon_a^2}{\cosh^2(\delta_x)} - \frac{\epsilon_i^2}{\delta_x\sinh(\delta_x)\cosh(\delta_x)}\right)\right] + \mathrm{O}(\epsilon^4) \tag{64}$$

For very short waves ($\delta_x \gg 1$), these relations simplify to:

$$\delta_{z,i} \approx \delta_x - \epsilon^2, \quad \omega^2 \approx \delta_x$$

and we recover the frequency of short non hydrostatic waves $\omega^2 = \delta_x$ (or $\Omega = \sqrt{gk_x}$ in dimensional form) with a slightly modified vertical wave-number. MSW correspond to the blue curve in (3.a).

Marginally stable surface gravity waves. We proved in Section 3.3 that the ratio $R^2(\delta_x, \delta_z)$ is maximum and equal to 1/4 only when δ_z is imaginary. The relations (48a) and (48b) are simultaneously satisfied (gray curve in Fig. 2.d). Any triplet $(\delta_x, \delta_z, \omega)$ satisfying these two relations is an acceptable wave solution only if it also satisfies the boundary dispersion relation (40b). As a consequence, $\delta_x(\omega)$ and $\delta_{z,i}(\omega)$ can be obtained combining (48b) and (40b) (both relations are recalled below), then (48a) leads to the non-linear equation for ω given by (65a):

$$\delta_x = \frac{\epsilon_a}{\epsilon_i}\omega^2 \tag{48b}$$

$$\omega^2 = \frac{\delta_x^2\tanh(\delta_{z,i})}{\delta_{z,i}+\epsilon^2\tanh(\delta_{z,i})} \tag{40b}$$

$$\delta_x^2(\omega) - \delta_{z,i}^2(\omega) - \epsilon_i^2\frac{\delta_x^2(\omega)}{\omega^2} - \epsilon_a^2\omega^2 + \epsilon^4 = 0 \tag{65a}$$

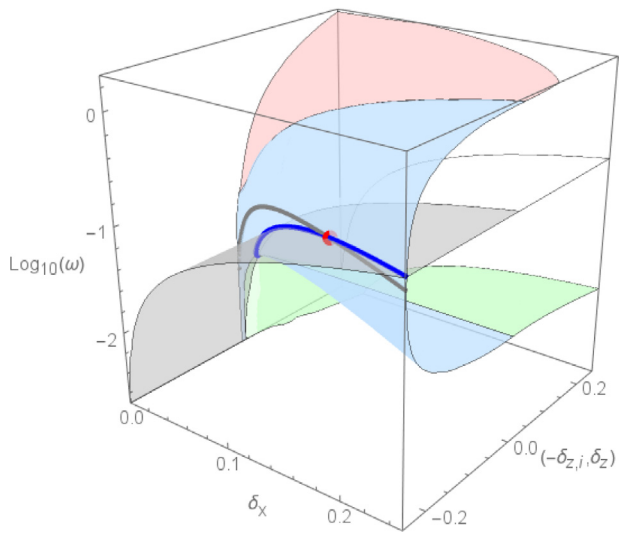

Fig. 5. Inner and boundary dispersion surfaces in $(\delta_x,\ \delta_z, \omega)$ space and wave solutions for long waves. Colors: (light red) acoustic wave region ($\delta_z^2 \geq 0 \& \omega$ large), (light blue) surface wave region ($\delta_z^2 \geq 0 \& \omega$ small), (light green) internal wave region ($\delta_z^2 < 0$), (white) boundary dispersion surface for $\delta_z \in \mathbb{R}$, (light gray) boundary dispersion surface for $\delta_z \in \mathbb{R}$. Blue curve: Modified Surface Waves (MSW). Gray curve: triplets $(\delta_x, \delta_z, \omega)$ satisfying (48b) and (48a). Red Point: marginally stable MSW Section 4.5.

For the stratification and acoustic parameters ϵ_i and ϵ_a given in Table 2, Eq. (65a) has a unique solution for $\omega_* \approx 0.154$. This wave solution (red point in Fig. 5) is marginally stable ($\omega_+ = \omega_-$ and $R^2(\delta_x, \delta_z) = 1/4$). Further investigations of this peculiar region of surface-wave phase-space must in particular take into account the consequences of earth rotation and wave non-linearity.

4.5. Long waves

We now prove the existence of two sub-branches of long wave solutions: mode-0 Modified Internal Modes (MIM-0) with horizontal wave-numbers in the range $\delta_x \in [0, \delta_{x,0}]$ and Long Modified Surface Waves (LMSW) in the range $\delta_x \in [\delta_{x,0}, +\infty)$.

Dispersion relations for long waves. Here, we perform specific developments for long waves where the vertical profile is almost depth-independent $|\delta_z| \approx 0$, δ_z being either real or purely imaginary (Fig. 3b). This corresponds to the long-wave part of the acoustic-gravity branch located in the region $\delta_z^2 \in (-\infty, \delta_{z,m=1}^2]$ of Fig. 4a.

Inserting the boundary dispersion relation (35b) into the inner dispersion relation (35a) and making a second-order Taylor expansion in δ_z leads to:

$$\delta_z^2(\delta_x) = \delta_{z,long}^2(\delta_x) = \left(\delta_{x,0}^2 - \delta_x^2\right) \frac{1 + \epsilon_i^2/3 - \epsilon_a^2}{(1+\epsilon_i^2/3)(1+\epsilon_i^2/3) - \delta_x^2\epsilon_a^2/3} + \mathrm{O}(\delta_z^4) \tag{66}$$

$\delta_{x,0}$ is the value of δ_x for which $\delta_z = 0$ is a solution of the inner and boundary dispersion relations (Section 2.6). At first order in ϵ^2, $\delta_{x,0}$ is equal to ϵ_i. The corresponding frequency can be obtained by inserting the approximation of the vertical wave-number given by (66) into the boundary relation dispersion (35b). An approximation at second order in δ_x^2 and ϵ^2 is:

$$\omega^2(\delta_x) = \omega_{long}^2(\delta_x) = \delta_x^2 \left(1 - \frac{1}{6}\left(\epsilon_i^2 + 3\epsilon_a^2\right) + \frac{1}{3}\epsilon_a^2\epsilon^2 + \frac{1}{45}\epsilon_i^4 + \mathrm{O}(\epsilon^6)\right) + \mathrm{O}(\delta_x)^4. \tag{67}$$

We also define:

$$\delta_{z,0}^2(\delta_x = 0) = \frac{\delta_{x,0}^2(1 + \epsilon_i^2/3 - \epsilon_a^2)}{(1+\epsilon_i^2/3)(1+\epsilon_i^2/3) - \delta_x^2\epsilon_a^2/3} + \mathrm{O}(\delta_z^4) \tag{68}$$

Fig. 6 shows the evolution of δ_z^2, $|\delta_z|$ and ω as functions of δ_x for long waves (6a, b and d) and for short and intermediate waves (6c).

$\boldsymbol{\delta_x \leq \delta_{x,0}}$. For $\delta_x \leq \delta_{x,0} \approx \epsilon_i$, the vertical wave-number δ_z given by (66) is real. This implies that $\omega^2 \approx \delta_x^2 \leq \epsilon_i\,\delta_x \leq \frac{\epsilon_i}{\epsilon_a}\delta_x$ (since $\epsilon_a < 1$) and, thus, using the bounds on ω_-^2, ω_+^2 given by (45), that these waves are always issued from the internal-wave region of the inner dispersion surface (ω_-^2), not from the acoustic-wave region (ω_+^2). In other words, there is no intersection between the boundary dispersion relation and the (real) acoustic-wave region for $\delta_z \in \mathbb{R}$ close to zero for the chosen boundary conditions . This is consistent with the fact that (acoustic) Lamb waves can only be solutions for different surface or bottom boundary conditions in Section 2.6.

Dukowicz (2013) notes that this wave solution, like any higher internal modes, has its frequency ω^2 approximately bounded by ϵ_i^2 (i.e. $\Omega \leq N$), since $\omega^2 \approx \delta_x^2 \leq \epsilon_i^2$. We however avoid to refer to this n=0 internal mode (MIM-0) as a barotropic wave. Indeed if $\epsilon_i = \epsilon_a = 0$, i.e. if stratification and compressibility vanish in this sub-branch disappears. Since $\delta_z \in \mathbb{R}$, MIM-0 propagates in the vertical direction but its vertical wave-number remains small even in strongly-stratified regions (large values of ϵ_i, see Table 6).

$\boldsymbol{\delta_x \geq \delta_{x,0}}$. For $\delta_x \geq \delta_{x,0}$ (but still small), δ_z given by (66) is purely imaginary. These long waves originate from the surface-wave branch MSW and will here be named LMSW. When δ_x increases, $\delta_{z,long}$ (66) converges to $\delta_{z,lmsw}$ (63), which is a better approximation for medium and short surface waves. Fig. 6.(a) shows δ_z^2 as a function of δ_x (for $\delta_x \leq 2\epsilon_i$). The two approximations given by (66), accurate for long waves, and (63), accurate for medium/short waves, are plotted. On Fig. 6.(b), the modulus of the vertical wave-number is shown on the same interval for δ_x (for $\delta_x \leq 2\epsilon_i$).

Fig. 6.c and d present the frequency ω as a function of the horizontal wave-number δ_x according to different approximations for small, intermediate and long horizontal wave-numbers. ω_{long} and ω_{msw} are computed by inserting the corresponding approximations (66) and (63) of δ_z in the boundary dispersion relation (35b). $\omega = \delta_x$ (resp. $\omega = \sqrt{\delta_x}$) represents the classical long shallow-water waves (resp. short non-hydrostatic surface waves) approximation. $\omega = \omega_{sw} = \sqrt{\delta_x \tanh(\delta_x)}$ is the frequency of an homogeneous and incompressible (non hydrostatic) ocean. Unsurprisingly, this last approximation is accurate over the full range of horizontal wave-numbers, even for the set of compressible stratified equations. Indeed, even if for long waves, δ_z is not directly linked to δ_x (in particular δ_z does not vanish for $\delta_x \approx 0$), δ_z remains small (less than ϵ_i) and thus $\delta_z/\tan(\delta_z)$ is close to 1.

Interestingly, and contrary to conclusions in Dukowicz (2013), the MIM-0 frequency cannot saturate at the buoyancy frequency for increasing horizontal wave-number δ_x but transforms into a vertically evanescent surface wave, whereas its vertical wave-number switches from real to purely imaginary.

Hydrostaticity and asymptotic behaviour. Surface edge waves are consequently either MIM-0 Modes ($\delta_z \in \mathbb{R}$ and $\delta_x < \delta_{x,0}$) or Modified Surface Waves (MSW, $\delta_z \in i\mathbb{R}$ and $\delta_x > \delta_{x,0}$). For $\delta_x = \delta_{x,0}$, a depth-independent gravity surface wave studied in Section 2.6 separates these two sub-branches. In the long wave approximation, the "long wave solution" (63) is an accurate approximation of both MIM-0 and LMSW.

We now further prove that *in the long-wave, low- frequency limit*:

- for $\delta_x < \delta_{x,0}$, the MIM-0 is (quasi-) hydrostatic and converges towards the $\sqrt{gH}$-phase-velocity shallow-wave solution (SHW) when stratification loosens (i.e. when $\epsilon_i \to 0$),
- for $\delta_x > \delta_{x,0}$, the LMSW solution remains non-hydrostatic and converges towards the other $\sqrt{gH}$-phase-velocity long-swell solution (LSW) when stratification loosens (i.e. when $\epsilon_i \to 0$).

The SHW and LSW asymptotic solutions are recalled in Table 1 and discussed in Section 2.6.

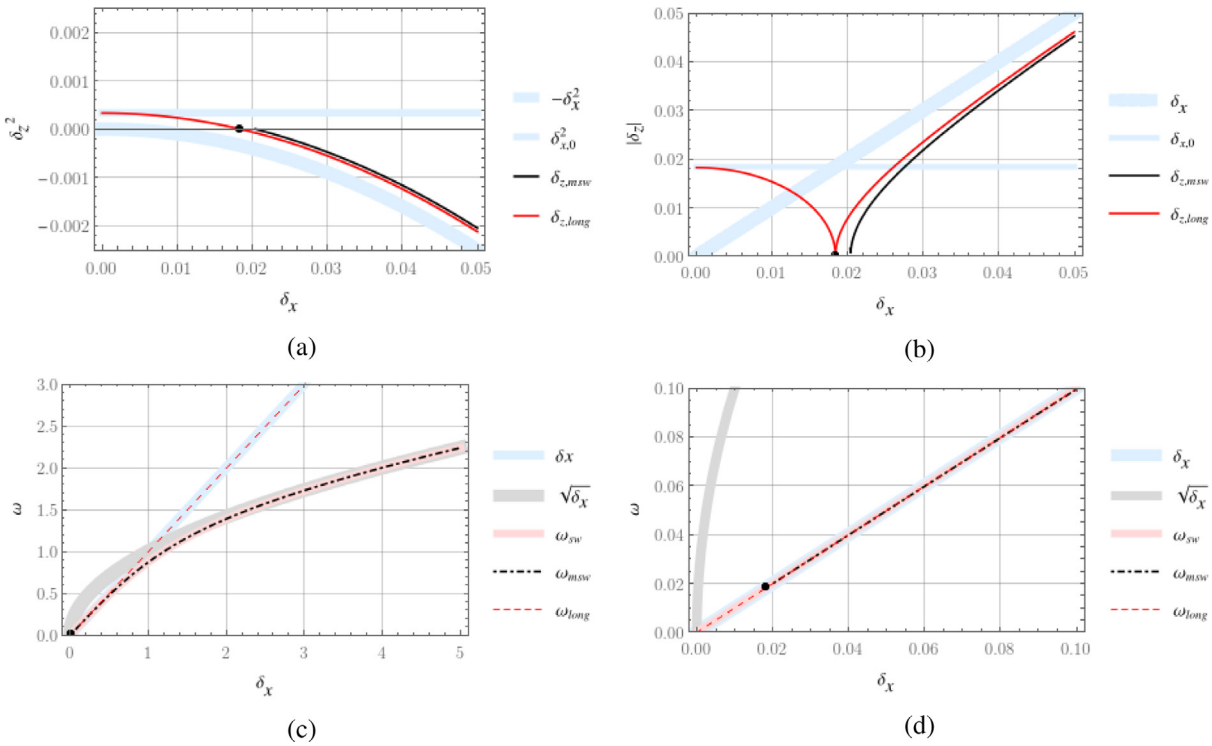

Fig. 6. Dispersion curves for (intermediate) and long wave-lengths δ_z. Black point: depth-independent surface gravity wave. Section 2.6.
(a) square modulus of the vertical wave-number δ_z^2 as a function of the horizontal wave-number δ_x. The exact solution can be numerically computed (not shown) and is visually not distinguishable from the blue curve (accurate approximation). The vertical wave-number of an incompressible and homogeneous ocean would follow the straight line $\delta_z = \delta_x$.
(b) modulus of the vertical wave-number $|\delta_z|$ as a function of the horizontal wave-number δ_x. The exact solution can be numerically computed (not shown) and is visually not distinguishable from the blue curve (accurate approximation). The vertical wave-number of an incompressible and homogeneous ocean would follow the straight line $\delta_z = \delta_x$.
(c) Frequency ω as a function of δ_x the horizontal wave-number for different approximations (short, intermediate and long waves).
(d) Frequency ω as a function of δ_x but in the vicinity of the origin.

Using the approximate solution for long waves (66) and for LMSW (63), we can compute their respective aspect-ratio:

$$r_{long}^2(\delta_x) = \frac{\delta_x^2}{\delta_{z,long}^2} = \delta_x^2 \frac{1+\epsilon_i^2/3-\epsilon_a^2}{(1+\epsilon_i^2/3)(1+\epsilon_i^2/3)-\delta_x^2\epsilon_a^2/3} + O(\delta_z^4) \tag{69a}$$

$$r_{msw}^2(\delta_x) = \frac{\delta_x^2}{\delta_{z,msw}^2} = \frac{\delta_x}{\epsilon_a^2 \tanh^2(\delta_x) - \delta_x \tanh(\delta_x) + \epsilon_i^2} \tag{69b}$$

Fig. 7 shows the evolutions of these aspect ratios as functions of the horizontal wave-number. A study of the variations of r_{long} shows that this ratio increases monotonically from 0 to infinity when δ_x varies from 0 to $\delta_{x,0}$ and decreases monotonically from infinity to 1 when δ_x varies from $\delta_{x,0}$ to infinity. In this latter range, r_{msw} remains close to r_{long}. Except in the vicinity of $\delta_{x,0}$, the aspect ratio r_{long} remains lower than 1 and it decreases monotonically to 0 when δ_x approaches 0. In this (very) long-wave range, the MIM-0 solution is thus hydrostatic and the dispersion relations (66) and (64) are approximately given by:

$$\delta_z^2 = \delta_{z,0}^2 \approx \epsilon_i^2 \quad \& \quad \omega^2 \approx \delta_x^2 \tag{70}$$

This solution is also the long-wave approximation of the hydrostatic wave solution (Appendix B).

The second branch is a monotonic function for $\delta_x \in [\delta_{x,0}, +\infty)$ and it decreases to 1 when $\delta_x \to +\infty$. As a consequence, it remains superior to 1 in this range of wave-numbers, the corresponding wave solution is non-hydrostatic and the dispersion relations (66) and (64) are approximately given by:

$$\delta_{z,i}^2 \approx \delta_x^2 - \epsilon_i^2 \quad \& \quad \omega^2 \approx \delta_x^2 \tag{71}$$

This solution is also the long-wave approximation of the non-hydrostatic wave solution (Appendix B).

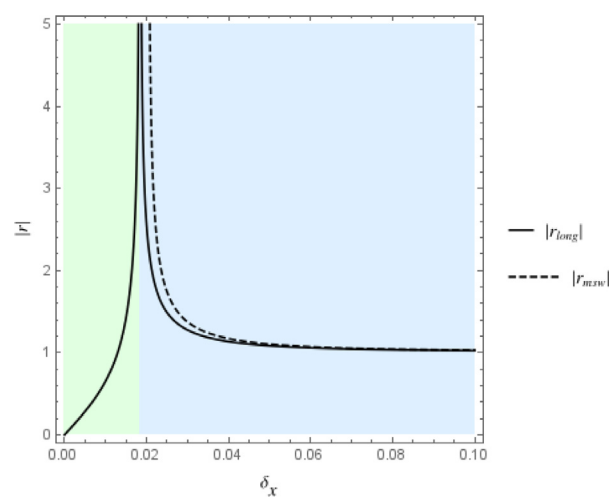

Fig. 7. Modulus of the wave aspect ratios r_{mim0} (black-solid curve) and r_{msw} (black, dashed curve). Colors: (light-green) internal wave region ($\delta_z \in \mathbb{R}$),(light-blue) surface wave ($\delta_z \in i\mathbb{R}$).

4.6. Summary: waves solutions in a bounded ocean

Unlike in an unbounded ocean, acoustic-gravity wave solutions in a bounded, free-surface ocean must satisfy both the inner and boundary dispersion relations. This induces the appearance of poles in these dispersion relations for $\delta_z = \frac{\pi}{2} + (m-1)\pi$ (MAM) and for $\delta_z = n\pi$ (MIM) with $(m,n) \in \mathbb{N}^* x \mathbb{N}^+$. For $\delta_z \in i\mathbb{R}$, the boundary dispersion relation does not exhibit any pole.

Table 5
Compressibility and stratification induced modifications to the usual dispersion relations given in table Table 1. The orders of magnitude of the modifications of the frequency and vertical wave-numbers (last column) are computed for the values of the main parameters given in table Table 2, $k_x = k_z = 1/H = 1/4000\ m^{-1}$, $m = 0$ and $n = 1$. The vertical wave-numbers of MIM-0 and LMSW are respectively compared to the vertical wave-numbers of SHW (0) and LSW (k_x).

Waves	frequency (Ω)	Vertical wave-number (k_z)	Modification (%)
Modified Acoustic Modes (MAM) $k_{z,m} = \frac{1}{H}(\pi/2 + m\pi), m \geq 0$ Section 4.3.2	$\Omega^2_{mam} = c_s^2(k_x^2 + k_z^2)\left[1 - \frac{g}{Hc_s^2}\frac{k_x^2 - k_{z,m}^2}{(k_x^2 + k_{z,m}^2)^2} + \frac{N^2}{gH}\frac{1}{k_x^2 + k_{z,m}^2}\right]$	$k_{z,m}\left[1 - \frac{g}{Hc_s^2}\frac{k_x^2 - k_{z,m}^2}{2(k_x^2 + k_{z,m}^2)k_{z,m}^2} + \frac{N^2}{2gH^2}\frac{1}{k_{z,m}^3}\right]$ (61)	(0.24, 0.16)
Modified Internal Modes (MIM) $k_{z,n} = \frac{1}{H}(n\pi), n \geq 1$ Section 4.3.1	$\Omega^2_{mim} = \frac{N^2 k_x^2}{k_x^2 + k_{z,n}^2}\left[1 - 2\frac{N^2}{gH}\frac{k_{z,n}^2}{(k_x^2 + k_{z,n}^2)^2}\right]$	$k_{z,n}\left[1 + \frac{N^2}{gH}\frac{1}{k_x^2 + k_{z,n}^2} + \left(\frac{N^2}{gH}\right)^3\frac{(k_x^2 - k_{z,n}^2)}{(k_x^2 + k_{z,n}^2)^3}\right]$	($-6.8\text{x}10^{-3}$, $3.8\text{x}10^{-3}$)
Modified Surface Waves (MSW) $k_x \geq k_{x,0} \approx \frac{N^2}{g}$ Section 4.4	$\Omega^2 = gk_x \tanh(Hk_x)$ (64)	$ik_x\sqrt{1 - \frac{1}{k_x}\left(\frac{N^2}{g\tanh(Hk_x)} + \frac{g}{c_s^2}\tanh(Hk_x)\right)}$	
Modified Internal Mode 0 (MIM-0) $k_x \leq k_{x,0} \approx \frac{N^2}{g}$ Section 4.5	$\Omega^2 = gHk_x^2\left[1 - \frac{1}{6}\left(\epsilon_i^2 + 3\epsilon_a^2\right)\right]$ (67)	$\sqrt{k_{x,0}^2 - k_x^2}$ (66)	(-0.88, $2.5\text{x}10^{-2}$)
Long Modified Surface Waves (LMSW) $k_x \geq k_{x,0} \approx \frac{N^2}{g}$ Section 4.5	$\Omega^2 = gHk_x^2\left[1 - \frac{1}{6}\left(\epsilon_i^2 + 3\epsilon_a^2\right)\right]$ (67)	$i\sqrt{k_x^2 - k_{x,0}^2}$ (66)	(-0.88, $-8.3\text{x}10^{-6}$)

A stratified ocean can propagate two types of surface edge waves:

- for medium and short wave-lengths ($\delta_x > \delta_{x,0}$), MSW are non-hydrostatic ($r_{lmsw} > 1$), evanescent ($\delta_{z,sw} \in i\mathbb{R}$) and converge towards the $\sqrt{gH}$-phase-velocity, depth-dependent ($\delta_x = \delta_{z,i}$) wave solution (LSW) when both $\epsilon_i \to 0$ and $\delta_x \to \delta_{x,0}$. Vertical variations of pressure are non-hydrostatic and in a homogeneous ocean, LMSW solutions remain depth-dependent ($\delta_x = \delta_{z,i} \neq 0$).
- for longer waves ($\delta_x < \delta_{x,0}$), MIM-0 are quasi-hydrostatic ($r_{mim0} < 1$ if δ_x is not in the neighbourhood of $\delta_{x,0}$), vertically propagating ($\delta_z \in \mathbb{R}$) and converges towards the shallow-water $\sqrt{gH}$-phase-velocity solution (SHW) when both $\epsilon_i \to 0$ and $\delta_x \to 0$. In this case, vertical variations of pressure are hydrostatic and LMIW solutions are depth-independent ($\delta_z = 0$). When the stratification loosens ($\epsilon_i \to 0$), the range of validity of MIM-0 solution ($0 < \delta_x < \delta_{x,0} \approx \epsilon_i$) shrinks to zero.

The frequency of acoustic wave solutions (modified by gravity) remains larger than $\omega_{c,a} = \epsilon^2/\epsilon_a$ whereas the frequency of gravity waves (modified by compressibility) remains smaller than $\omega_{c,i} = \epsilon_i$ (Section 3.3).

Table 5 summarizes the main approximations for the different type of waves (acoustic, gravity and surface waves/modes) given in this paper. These approximations are indicated in their dimensional form. For sake of readability, some of the relations given in Table 5 are lower order versions of our derivations. They generally stem from first-order correction terms, compared with usual dispersion relations introduced in Table 1. In that case, a red link to the higher approximation is given.

Table 6 gives orders of magnitude of various characteristics of these acoustic gravity waves for the reference set of (ϵ_a, ϵ_i) parameters (Table 2) and for a shallow or a strongly stratified ocean.

For the 4000 m-deep reference ocean, the horizontal length scale associated with the transformation of the MSW into the long MIM ($\lambda_{x,lmsw} = 2\pi/(\delta_{x,lmsw}/4000)$) reaches 1367 km against 62 km for the same 10 m-deep ocean. When δ_x decreases below $\delta_{x,lmsw}$, δ_z increases monotonically to a maximum value $\delta_{z,lmsw}(\delta_x = 0)$. This vertical length scale reaches 1379 km for the 4000 m-deep reference ocean and 62 km for the same 10 m-deep ocean. A rule can be formulated as: the longer the horizontal length scale of the oscillation, the shorter its vertical length scale; and the weaker the stratification (vanishing ϵ_i) the longer its horizontal length-scale $\lambda_{x,lmsw}$. This long MIM solution is a low-frequency oscillation of the ocean due to gravity and associated with ocean stratification. It disappears when stratification vanishes and the ocean becomes an homogeneous layer of water. It does persist in an incompressible ocean but is slightly modified by compressibility.

Table 6
Orders of magnitude of various scales. Notations refer to non-dimensional variables whereas orders of magnitude are given for dimensional quantities. Parameters for the "*Reference*" ocean are given in table Table 2. "*10-m-deep*" ocean is a 10-m-deep *Reference* ocean whereas a "$N = 5\text{x}10^{-3}$ s^{-1}" ocean is a reference ocean with $N = 5\text{x}10^{-3}$ s^{-1}.

	Notation	*Reference*	*10-m-deep*	$N = 5\text{x}10^{-3}$ s^{-1}
Parameters	ϵ_a	0.13	$6.6\text{x}10^{-3}$	0.13
	ϵ_i	$2.0\text{x}10^{-2}$	$1.0\text{x}10^{-3}$	0.1
Acoustic cut-off	$2\pi\sqrt{H/g}/\omega_{c,a}$	31.3 min	31.3 min	20 min
Internal cut-off	$2\pi\sqrt{H/g}/\omega_{c,i}$	1.7 h	1.7 h	21 min
Depth-independent surface gravity wave	$2\pi H/\delta_{x,0}$	1367 km	62 km	247 km
	$2\pi\sqrt{H/g}/\omega_0$	1.9 h	1.7 h	21 min
MIW, $\delta_z(0)$	$2\pi H/\delta_{z,0}$	1380 km	62 km	250 km
	$2\pi\sqrt{H/g}/\omega_{z,0}$	∞	∞	∞
MSW, marginally-stable wave	$2\pi H/\delta_{x,*}$	162 km	408 m	25 km
	$2\pi H/\delta_{z,*}$	164 km	408 m	25 km
	$2\pi\sqrt{H/g}/\omega_*$	13.7 min	41.6 s	2.4 min

5. Discussion, conclusion

An Eulerian, analytical model for acoustic gravity waves propagating in a compressible, stratified, free-surface, non-rotating ocean has been derived and investigated with several objectives: recover acoustic waves and modes in a unified dispersion model, describe analytically the modifications of the characteristics of these waves and modes for small changes in compressibility or stratification and, finally, anticipate the impact of compressibility in the new generation of non-hydrostatic, compressible, ocean models (Auclair et al., 2018).

An original investigation (at least to the authors' knowledge) based on 3D graphics in (δ_x, δ_z, ω) phase-space has been carried out to support and illustrate the analytical developments. Well-known acoustic and internal modes (MAM and MIM) have in particular been recovered and have been associated to the infinite number of discrete poles of the

inner and boundary dispersion relations. A least two peculiar regions of the phase space have been investigated in more detail. Firstly, the long acoustic gravity wave branch has indeed been decomposed in two sub-branches: one associated to a modified mode-0 internal mode (MIM-0) with a real vertical wave-number, the other to a modified long surface gravity wave (LMSW) with imaginary vertical wave-number. Secondly, modified surface gravity waves (MSW) have been shown to be marginally stable for intermediate wave-numbers in a region of phase space where compressibility and stratification induced effects approximately compensate.

Analytical solutions are given in dimensional form in Appendix C, such solutions can conveniently be used to validate non-hydrostatic, compressible, free-surface ocean models (Auclair et al., 2018).

Declaration of competing interest

The authors declare that they have no known competing financial interests or personal relationships that could have appeared to influence the work reported in this paper.

Acknowledgments

We greatly thank the computer service of the *Laboratoire d'Aérologie* for NUWA, our laboratory cluster. The present study has been supported by French-Navy SHOM contract *GIBRALTAR*, by LEFE contract *GEPETO*, by ANR grant *SOLAB*, by IDEX Chair of attractivity *TEASAO* and by H2020 contract *IMMERSE*.

Appendix A. Mathematical demonstrations

A.1. δ_z real or purely imaginary

In this section, we prove that under the condition of smallness of parameters ϵ_i and ϵ_a, δ_z is either real or imaginary and thus that the frequency ω is real.

Polarization function in s-coordinates. The eigenvalue problem (28) and the surface boundary condition (28b) are rewritten in non-dimensional form as:

$$G''(s) + \delta_z^2 G(s) = 0 \tag{A.1}$$

$$G(1) = 1 \tag{A.2}$$

$$G(0) = 0 \tag{A.3}$$

$$G'(1) + \left(\frac{\epsilon_i^2 + \epsilon_a^2}{2} - \frac{\delta_x^2}{\omega^2}\right) G(1) = 0 \tag{A.4}$$

where $s = \frac{z+H}{H}$, $G(s(z)) = F(z)$ and $\epsilon_i^2 = \frac{N^2 H}{g}, \epsilon_a^2 = \frac{gH}{c_s^2}, \delta_x = k_x H, \delta_z = k_z H, \omega = \Omega\sqrt{\frac{H}{g}}$.

Energy equation. δ_z is linked to δ_x and ω by the inner dispersion relation

$$\delta_z^2 = \left(\delta_x^2 \frac{\epsilon_i^2 - \omega^2}{\omega^2} + \epsilon_a^2\omega^2 - \frac{(\epsilon_i^2 + \epsilon_a^2)^2}{4}\right) \tag{A.5}$$

Multiplying (A.1) by $\overline{G(s)}$ and integrating over $[0,1]$ we get:

$$\int_0^1 G''(s)\overline{G(s)}\mathrm{d}s + \delta_z^2 \int_0^1 |G(s)|^2 \mathrm{d}s = 0$$

Integration by parts leads to:

$$-\int_0^1 |G'(s)|^2 \mathrm{d}s + \delta_z^2 \int_0^1 |G(s)|^2 \mathrm{d}s + G'(1)\overline{G(1)} - G'(0)\overline{G(0)} = 0$$

and using (A.2), (A.3), (A.4)

$$\delta_z^2 \int_0^1 |G(s)|^2 \mathrm{d}s + \left(\frac{\delta_x^2}{\omega^2} - \frac{\epsilon_i^2 + \epsilon_a^2}{2}\right) = \int_0^1 |G'(s)|^2 \mathrm{d}s$$

Using the Poincaré inequality $\int_0^1 |G(s)|^2 \mathrm{d}s \le \int_0^1 |G'(s)|^2 \mathrm{d}s$ and $1 = |G(1)|^2 \le \int_0^1 |G'(s)|^2 \mathrm{d}s$, we obtain:

$$\delta_z^2 \mu + \left(\frac{\delta_x^2}{\omega^2} - \frac{\epsilon_i^2 + \epsilon_a^2}{2}\right) \nu = 1 \tag{A.6}$$

with $0 \le \mu \le 1$ and $0 \le \nu \le 1$.

Imaginary part of the energy equation. Taking the imaginary part of (A.6) and using (A.5)

$$\mu\left(\epsilon_a^2 \Im[\omega^2] + \delta_x^2 \epsilon_i^2 \Im[1/\omega^2]\right) + \nu \delta_x^2 \Im[1/\omega^2] = 0$$

or, using $\Im[1/\omega^2] = -\Im[\omega^2]/|\omega|^4$,

$$\Im[\omega^2]\left(\mu\left(\epsilon_a^2 - \epsilon_i^2 \frac{\delta_x^2}{|\omega|^4}\right) - \nu \frac{\delta_x^2}{|\omega|^4}\right) = 0 \tag{A.7}$$

Let us assume that ω is neither real or imaginary. This implies $\Im[\omega^2] \neq 0$ and (A.7) leads to:

$$\mu\left(\epsilon_a^2 \frac{|\omega|^4}{\delta_x^2} - \epsilon_i^2\right) - \nu = 0 \tag{A.8}$$

We will show below that, in this case, solutions can exist only for non physical values of ϵ_i, ϵ_a satisfying $\max(\epsilon_i, \epsilon_a) > \sqrt{2}$.

Real part of the energy equation. Taking the real part of (A.6)

$$\mu\left(-\delta_x^2 + \delta_x^2 \epsilon_i^2 \Re[1/\omega^2] - \frac{(\epsilon_i^2 + \epsilon_a^2)^2}{4} + \epsilon_a^2 \Re[\omega^2]\right) + \nu\left(\delta_x^2 \Re[\frac{1}{\omega^2}] - \frac{\epsilon_i^2 + \epsilon_a^2}{2}\right) = 1 \tag{A.9}$$

or, using $\Re[1/\omega^2] = \Re[\omega^2]/|\omega|^4$,

$$\mu\left(-\delta_x^2 - \frac{(\epsilon_i^2 + \epsilon_a^2)^2}{4} + (\frac{\delta_x^2 \epsilon_i^2}{|\omega|^4} + \epsilon_a^2)\Re[\omega^2]\right) + \nu\left(\frac{\delta_x^2}{|\omega|^4}\Re[\omega^2] - \frac{\epsilon_i^2 + \epsilon_a^2}{2}\right) = 1. \tag{A.10}$$

(A.8) allows to simplify in:

$$\mu\left(-\delta_x^2 - \frac{(\epsilon_i^2 + \epsilon_a^2)^2}{4} + 2\epsilon_a^2 \Re[\omega^2]\right) - \nu\left(\frac{\epsilon_i^2 + \epsilon_a^2}{2}\right) = 1 \tag{A.11}$$

Energy-based system of equations. Eqs. (A.8) and (A.11) can be summarized in

$$\begin{aligned} \alpha\mu - \beta\nu &= 1 \\ \gamma\mu - \nu &= 0 \end{aligned} \tag{A.12}$$

with

$$\alpha = -\delta_x^2 - \frac{(\epsilon_i^2 + \epsilon_a^2)^2}{4} + 2\epsilon_a^2 \Re[\omega^2], \beta = \frac{\epsilon_i^2 + \epsilon_a^2}{2}, \gamma = \epsilon_a^2 \frac{|\omega|^4}{\delta_x^2} - \epsilon_i^2$$

Using $\beta > 0$, it is easy to check that (A.12) has solutions (μ, ν) positive and with magnitude less than one only if

$\gamma > 1$ and $\alpha > (1+\beta)\gamma$

or

$0 \le \gamma \le 1$ and $\alpha \ge 1 + \beta\gamma$

The conditions above immediately exclude the cases $\epsilon_a = 0$ (which leads to $\gamma < 0$) and $\Re[\omega^2] \le 0$ (which leads to $\alpha < 0$). They will not be considered below.

First case: $0 \le \gamma \le 1$. This implies:

$$|\omega|^4 \le \frac{\delta_x^2}{\epsilon_a^2}(1+\epsilon_i^2) \tag{A.13}$$

$\alpha \ge 1+\beta\gamma$ writes:

$$\Re[\omega^2] \ge \frac{1}{2\epsilon_a^2}\left[1+\delta_x^2+\frac{(\epsilon_a^2+\epsilon_i^2)^2}{4}+\frac{\epsilon_i^2+\epsilon_a^2}{2}\left(\epsilon_a^2\frac{|\omega|^4}{\delta_x^2}-\epsilon_i^2\right)\right]$$

Now using the inequalities $|\Re[\omega^2]|^2 \le |\omega|^4$ and (A.13), we get

$$\begin{aligned}\frac{\delta_x^2}{\epsilon_a^2}(1+\epsilon_i^2) &\ge |\omega|^4 \\ &\ge \left(\frac{1}{2\epsilon_a^2}\left[1+\delta_x^2+\frac{(\epsilon_a^2+\epsilon_i^2)^2}{4}+\frac{\epsilon_i^2+\epsilon_a^2}{2}\left(\epsilon_a^2\frac{|\omega|^4}{\delta_x^2}-\epsilon_i^2\right)\right]\right)^2\end{aligned} \tag{A.14}$$

Using a computing algebra software to simplify the technical exercice, we can prove that (A.14) has solutions if and only if

$$\epsilon_i^2 > \sqrt{4+\epsilon_a^4}$$

which requires $\epsilon_i > \sqrt{2}$.

Second case: $\gamma > 1$. This implies:

$$|\omega|^4 > \frac{\delta_x^2}{\epsilon_a^2}(1+\epsilon_i^2) \tag{A.15}$$

$\alpha > (1+\beta)\gamma$ can be written as:

$$\gamma < \frac{\alpha}{1+\beta}$$

or

$$|\omega|^4 < \frac{\delta_x^2}{\epsilon_a^2}\left[\epsilon_i^2+\frac{1}{1+\frac{\epsilon_a^2+\epsilon_i^2}{2}}\left(-\delta_x^2-\frac{(\epsilon_i^2+\epsilon_a^2)^2}{4}+2\epsilon_a^2\Re[\omega^2]\right)\right]$$

Now using $0 \le \Re[\omega^2] \le |\omega|^2$ and adding (A.15), we get:

$$\frac{\delta_x^2}{\epsilon_a^2}(1+\epsilon_i^2) < |\omega|^4 < \frac{\delta_x^2}{\epsilon_a^2}\left[\epsilon_i^2+\frac{1}{1+\frac{\epsilon_a^2+\epsilon_i^2}{2}}\left(-\delta_x^2-\frac{(\epsilon_i^2+\epsilon_a^2)^2}{4}+2\epsilon_a^2|\omega|^2\right)\right]$$

which has non trivial solutions if and only if

$$\epsilon_a^2 > 2+\epsilon_i^2$$

which requires $\epsilon_a > \sqrt{2}$.

Conclusion. This concludes the proof. If $\epsilon_a = 0$ or $\max(\epsilon_i, \epsilon_a) \le \sqrt{2}$, then $\Im[\omega^2]$ is zero. This also leads to $\Im[\delta_z^2] = 0$ and we conclude that, under these conditions, δ_z is either real or purely imaginary. Eq. (A.10) with μ and ν positive further show that $Re[\omega^2] \ge 0$ implying that ω can only be real and the amplitude of the wave solution does not diverge in time.

A.2. Vanishing ratio $R^2(\delta_x, \delta_z)$

We now show that the two roots $\omega_\pm$ are well-separated except when
(i) δ_z is imaginary and close to $\delta_z = i\delta_{z,i,*} = i\left(\epsilon_a^2-\epsilon_i^2\right)/2$,
(ii) δ_z is real and $\epsilon_i = \epsilon_a \& \delta_z = 0$

δ_z Real. The ratio of reference functions $R^2(\delta_x, \delta_z)$, defined by (43), depends indeed on two variables $(\delta_x,\ \delta_z)$ and two parameters $(\epsilon_i,\ \epsilon_a)$. A study of its variations for $\delta_x \in \mathbb{R}$ shows that, for non-vanishing $(\epsilon_i,\ \epsilon_a)$, it has an upper bound:

$$R^2_{max}(\delta_z) = \max_{\delta_x} R^2(\delta_x, \delta_z) = \frac{1}{4}\frac{\epsilon_a^2\epsilon_i^2}{\delta_z^2+\epsilon^4} \tag{A.16}$$

and this maximum value is attained for

$$\delta_x^2 = \delta_z^2+\epsilon^4. \tag{A.17}$$

Since for $max(\epsilon_i, \epsilon_a) \le \sqrt{2}$ or $\epsilon_a = 0$ the roots (44) are real (Appendix A.1), $R_{max}(\delta_z)$ must remain bellow 1/4 but approaches 1/4 for both a near depth-independent vertical profile (i.e. $\delta_z \approx 0$[3]) and $\epsilon_a \approx \epsilon_i$ (or in dimensional form $N = g/c_s$). This last equality is true when the stratification and the compressibility effects have an identical contribution to the vertical variation of background stratification $\hat{\rho}_h(z)$. In all other cases, the vast majority, the two roots are well separated and given by:

$$\omega_-(\delta_x,\ \delta_z) \approx \omega_i(\delta_x,\ \delta_z), \quad \omega_+(\delta_x,\ \delta_z) \approx \omega_a(\delta_x,\ \delta_z) \tag{A.18}$$

δ_z Imaginary. When horizontal and vertical wavenumbers are close together, the left-hand side and right-hand side of (40a) both vanish, i.e., the influence of stratification $(\epsilon_i^2\delta_x^2/\omega^2)$ and compressibility $(\epsilon_a^2\omega_a^2)$ cancel out. In other words, differences between horizontal and vertical wavenumbers are indication of the influence of ocean stratification and/or compressibility. In an incompressible, homogeneous (unstratified) ocean, $\epsilon_i = \epsilon_a = 0$ and vertical and horizontal wave-numbers are equal. The developments of ω_-^2, ω_+^2 for small ϵ_i, ϵ_a are identical to those for real vertical wavenumbers (51), (54) just replacing δ_z^2 by $-\delta_{z,i}^2$. The remaining question is that of root separation when $\delta_z \in i\,\mathbb{R}$. Unlike when $\delta_z \in \mathbb{R}$ (previous sub-section), the ratio $R^2(\delta_x,\ i\,\delta_{z,i})$ can be equal to 1/4 even when δ_z is not small. Relation (40a) imposes $0 \le \delta_{z,i}^2 \le \delta_x^2 + \frac{(\epsilon_a^2+\epsilon_i^2)^2}{4}$ and in this range of values, R^2 is an increasing function of $\delta_{z,i}^2$. The value of $R^2 = 1/4$ is attained for $\delta_{z,i}^2 = \delta_{z,i,\star}^2$ given by

$$\delta_{z,i,\star}^2 = \delta_x^2 + \frac{(\epsilon_a^2+\epsilon_i^2)^2}{4} - 2\epsilon_a\epsilon_i\delta_x, \tag{A.19}$$

for which the inner dispersion relation has a double root

$$\omega_+^2 = \omega_-^2 = \frac{\epsilon_i}{\epsilon_a}\delta_x \tag{A.20}$$

When $\delta_{z,i}$ is less than $\delta_{z,i,\star}$, the two roots become separated. Again, since we have proved in appendix that only solutions with real frequency can exist (when the domain is bounded), the case $\delta_{z,i}^2 > \delta_{z,i,\star}^2$, which would lead to $R^2 > 1/4$ can be excluded. Note that ω_-, ω_+ as functions of $\delta_{z,i}$ are not differentiable at the neutral point $\delta_{z,i} = \delta_{z,i,\star}$.

A.3. Internal and acoustic modes (MIM & MAM)

MIM solutions: we have shown in Section 3.4 that the root of the inner dispersion relation corresponding to internal gravity waves is well-approximated by ω_i^2. Making $\omega^2(\delta_x) \approx \omega_i^2$ in the boundary dispersion relation (35b) leads to

$$\frac{1}{\delta_z/\tan(\delta_z)+\frac{\epsilon_i^2+\epsilon_a^2}{2}} \approx \frac{\epsilon_i^2}{\delta_x^2+\delta_z^2+\frac{1}{4}\left(\epsilon_i^2+\epsilon_a^2\right)^2} \tag{A.21}$$

If we assume here that δ_z is not close to 0, the right-hand side of (A.21) is always small and thus $\delta_z/\tan(\delta_z)$ has to be large, i.e., the vertical wavenumber δ_z is close to $\delta_{z,n} \approx n\pi$ with n a non-zero integer. This agrees with the internal gravity wave solution found graphically in Section 4.2.

MAM solutions: we can now use the fact that the root of the inner dispersion relation corresponding to acoustic waves is well-approximated

[3] We use the term *depth-independent* even if $F(z)$ is a linear function of z when δ_z is close to 0 (see (29)), so that the vertical profile of $W(z)$ is approximately linear while the vertical profile of $U(z)$ is approximately constant.

by ω_a^2. Making $\omega^2(\delta_x) \approx \omega_a^2$ in the boundary dispersion relation (35b) leads to:

$$\delta_z/\tan(\delta_z) + \frac{\epsilon_i^2+\epsilon_a^2}{2} \approx \frac{\epsilon_a^2}{1+\left(\delta_z^2+\frac{1}{4}\left(\epsilon_i^2+\epsilon_a^2\right)^2\right)/\delta_x^2} \tag{A.22}$$

Since the right-hand side of (A.22) is small (bounded by ϵ_a^2), $\delta_z/\tan(\delta_z)$ has to be small and thus the vertical wavenumber δ_z is close to $\delta_{z,m} \approx \pi/2 + m\pi$, with $m \in \mathbb{N}$.

A.4. Surface waves existence

In the more general case of a stratified and compressible ocean, we now show the existence of solutions to (40a) and (40b) the dispersion relations for $\delta_z \in i\mathbb{R}$.

Let us define $f(\delta_x, \delta_{z,i})$ by:

$$f(\delta_x,\delta_{z,i}) = \delta_x^2 - \delta_{z,i}^2 - \left(\epsilon_i^2\frac{\delta_x^2}{\omega^2} + \epsilon_a^2\omega^2 - \frac{(\epsilon_a^2+\epsilon_i^2)^2}{4}\right),$$

$$\text{with } \omega^2 = \frac{\delta_x^2}{\frac{\delta_{z,i}}{\tanh(\delta_{z,i})} + \frac{\epsilon_a^2+\epsilon_i^2}{2}}$$

The inner boundary relation translates into $f(\delta_x, \delta_{z,i}) = 0$. We can check that, for a given $\delta_{z,i}$, $f(\delta_x, \delta_{z,i})$ is an increasing function of δ_x.[4] Let $\delta_{x,0}$ be the value of δ_x defined by $f(\delta_{x,0}, \delta_z = 0) = 0$ ($\delta_{x,0}$ will be given in (66), and is close to ϵ_i). In particular, we have $f(\delta_x, 0) \le f(\delta_{x,0}, 0) = 0$ for $\delta_x \le \delta_{x,0}$. We can also verify that for a given δ_x such that $\delta_x \le \delta_{x,0}$, the maximum of $f(\delta_x, \delta_z)$ is attained in $\delta_{z,i} = 0$. This proves that if $\delta_x < \delta_{x,0}$, $f(\delta_x, \delta_{z,i}) < 0$ $\forall \delta_{z,i}$. Therefore, modified surface waves can only exist under the condition $\delta_x \ge \delta_{x,0}$.

A.5. Surface waves: $\delta_{z,i} \approx \delta_x$

For small parameters ϵ_a and ϵ_i, we show in the present section that $\delta_{z,i}^2$ is close to δ_x^2 for any MSW solution.

We can show that $1 \le \frac{\delta_{z,i}}{\tanh(\delta_{z,i})} \le \delta_{z,i}^2+1$, $\forall \delta_{z,i} \in \mathbb{R}$. Injecting these two inequalities in the surface dispersion relation leads to:

$$\frac{\delta_x^2}{\omega^2} \le \delta_{z,i}^2 + 1 + \frac{\epsilon_a^2+\epsilon_i^2}{2}, \qquad \text{and} \qquad \omega^2 \le \delta_x^2$$

Since the inner dispersion relation implies $-\frac{(\epsilon_a^2+\epsilon_i^2)^2}{4} \le \delta_x^2 - \delta_{z,i}^2 \le \epsilon_i^2\frac{\delta_x^2}{\omega^2} + \epsilon_a^2\omega^2$, we finally get:

$$-\frac{(\epsilon_a^2+\epsilon_i^2)^2}{4} \le \delta_x^2 - \delta_{z,i}^2 \le \epsilon_i^2\delta_{z,i}^2 + \epsilon_a^2\delta_x^2 + \epsilon_i^2\left(1+\frac{\epsilon_a^2+\epsilon_i^2}{2}\right)$$

Using the smallness of the parameters ϵ_a and ϵ_i, we can then conclude that $\delta_{z,i}^2$ is indeed close to δ_x^2.

A.6. MIM-0 long-wave sub-branch

In the present section of the appendix, we show that the horizontal wave-number of the MIM-0 solution $(\delta_{x,mim0}(\delta_z),\ \omega_{mim0}(\delta_z))$ is a decreasing function of δ_z. It satisfies $\delta_{x,mim0}(0) = \delta_{x,0} \ge 0$ and $\delta_{x,mim0}(\delta_{z,0}) = 0$ for $\delta_{z,0} \in [0, \delta_{z,m=0} \approx \pi/2[$.

[4] This simple demonstration requires the assumption $\epsilon_a^2 \le 2 + \epsilon_i^2$, i.e., the same used in appendix to prove that the imaginary part of δ_z^2 is zero.

Wave solutions of MIM-0 type must satisfy both the inner and boundary dispersion relation ((35a) and (35b)) with $\delta_z \in \mathbb{R}$. We have also shown that MIM-0 is part of the internal branch and as a consequence approximately satisfies (42b). Substituting then (35b) into (42b) leads to a relation between the horizontal and vertical wave-numbers:

$$\delta_x^2 = \delta_{x,mim0}^2(\delta_z) = -\delta_z^2 - \epsilon^4 + \epsilon_i^2\left(\epsilon^2 + \delta_z\,\mathrm{cotan}(\delta_z)\right) \tag{A.23}$$

with $\delta_{x,mim0}^2(0) = \delta_{x,0}^2 = -\epsilon^4 + \epsilon_i^2\left(\epsilon^2+1\right)$. When $\delta_{x,0}^2 < 0$, this depth-independent solution does not propagate horizontally and we will assume in the following that $\delta_{x,0}^2 = -\epsilon^4 + \epsilon_i^2\left(\epsilon^2+1\right) \ge 0$. In Section 4.2, $\delta_{z,m=0}$ has been defined as a root of $\epsilon^2 + \delta_z\,\mathrm{cotan}(\delta_z)$ and when $\delta_z \to \delta_{z,m=0}^{(-)}$, $\delta_x^2(\delta_z) \to -\infty$. This means that there must exist $\delta_{z,0} \in [0, \delta_{z,m=0}[$ such that $\delta_{x,mim0}(\delta_{z,0}) = 0$ and $\delta_{z,0}$ satisfies:

$$-\delta_z^2 - \epsilon^4 + \epsilon_i^2\left(\epsilon^2 + \delta_z\,\mathrm{cotan}(\delta_z)\right) = 0 \tag{A.24}$$

We can additionally show that $\delta_{x,mim0}(\delta_z)$ is monotonic (decreasing) for $\delta_z \in [0, \delta_{z,0}]$. Indeed, its derivative

$$\frac{d\delta_{x,mim0}}{d\delta_z}(\delta_z) = 2\delta_z^2 + \epsilon_i^2\left(\delta_z - \mathrm{cotan}(\delta_z)\right) \tag{A.25}$$

is positive for $\delta_z \in [0, \delta_{z,0}]$ since it satisfies $\frac{d\delta_{x,mim0}}{d\delta_z}(0) = 0$ and is an increasing function of δ_z over this interval. The monotonicity of the derivative can be proven by computing the second order derivative

$$\frac{d^2\delta_{x,mim0}}{d\delta_z^2}(\delta_z) = 2 + 2\epsilon_i^2\frac{1-\delta_z\,\mathrm{cotan}(\delta_z)}{\sin^2(\delta_z)} \tag{A.26}$$

and using the Taylor series of $\mathrm{cotan}(z)$, we can further show that $(1 - \delta_z\,\mathrm{cotan}(\delta_z)) \ge 0$ and thus $\frac{d^2\delta_{x,mim0}}{d\delta_z^2}(\delta_z) \ge 0$.

A.7. Monotonicity of the branches of wave solutions ?

In the present section of the appendix, we show that the branches of acoustic wave solutions are monotonic and decreasing if ϵ_a and ϵ_i remain small.

To do so, the derivatives of δ_x^2 and ω^2 with respect to δ_z given respectively by (56a) and (56b) are computed:

$$\begin{aligned}\left(\epsilon^2 - J(\delta_z)\right)^2\frac{d\delta_x^2}{d\delta_z}(\delta_z) =& -2\delta_z J^2(\delta_z)\\ &+ 2\epsilon^2\delta_z^2 J'(\delta_z) + \epsilon_i^2 J^2(\delta_z)J'(\delta_z)\\ &+ 2\epsilon^4\delta_z - (\epsilon_i^4+\epsilon_i^2\epsilon_a^2)J(\delta_z)J'(\delta_z)\\ &+ \frac{1}{4}(\epsilon_a^6 - 2\epsilon_i^6 - 3\epsilon_i^4\epsilon_a^2)J'(\delta_z)\end{aligned} \tag{A.27a}$$

$$\begin{aligned}\left(\epsilon^2 - J(\delta_z)\right)^2\frac{d\omega^2}{d\delta_z}(\delta_z) =& \delta_z^2 J'(\delta_z) - 2\delta_z J(\delta_z)\\ &+ (\epsilon_a^2 - \epsilon_i^2)\delta_z^2\\ &+ \frac{1}{4}(\epsilon_a^4 - 3\epsilon_i^4 - 2\epsilon_a^2\epsilon_i^2)J'(\delta_z)\end{aligned} \tag{A.27b}$$

where

$$J(\delta_z) = \delta_z\ \mathrm{cotan}(\delta_z) \tag{A.28a}$$

$$J'(\delta_z) = \frac{\sin(2\delta_z) - 2\delta_z}{2\sin^2(\delta_z)} \le 0 \tag{A.28b}$$

Note that the relations above are not Taylor expansions of the derivatives with respect to ϵ_a and ϵ_i, they are exact relations. The derivative of δ_x^2 given by (A.27a) is negative at third order in $(\epsilon_a,\ \epsilon_i)$ whereas the derivative of ω^2 (A.27b) is negative only at first order in $(\epsilon_a,\ \epsilon_i)$. At higher order, (A.27a) and (A.27b) additionally show the values of δ_z for which δ_x^2 and ω^2 are monotonic depending of the values of this two parameters.

$\delta_x^2(\delta_z)$ and $\omega^2(\delta_z)$ are thus monotonously decreasing functions of δ_z if ϵ_a and ϵ_i remains small.

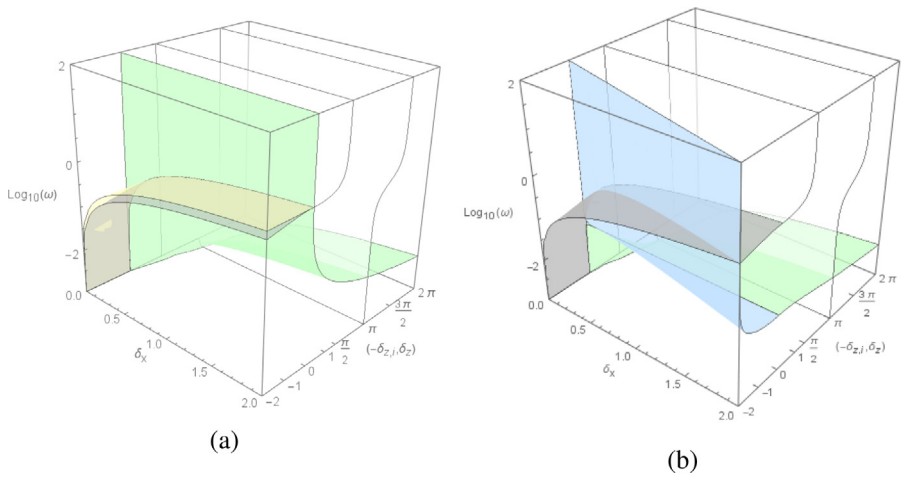

Fig. B.1. Inner and boundary dispersion surfaces in $(\delta_x,\ \delta_z,\ \omega)$ space and wave solutions for an incompressible ocean:
(a) hydrostatic assumption,
(b) non-hydrostatic assumption.
Colors: (light red) $\delta_z^2 \geq 0 \& \omega \geq 1$, (light green) $\delta_z^2 \geq 0 \& \omega < 1$, (light blue) $\delta_z^2 < 0$, (white) boundary dispersion surface for $\delta_z \in \mathbb{R}$, (light gray) boundary dispersion surface for $\delta_z \in i\mathbb{R}$, (light yellow) $\omega^2 = \delta_x^2$ barotropic wave.

Appendix B. Incompressible hydrostatic model & non-hydrostatic models

Hydrostatic & incompressible model. Under the hydrostatic assumption, the propagation relation (17) in a uniformly stratified, incompressible ocean turns to:

$$\tilde{W}''(z) + \frac{g}{D_0\ \omega}\tilde{W}(z) = 0 \tag{B.1}$$

associated to the surface and bottom boundary conditions:

$$\tilde{W}'(0) - \frac{gk_x^2}{\omega^2}\tilde{W}(0) = 0, \quad \tilde{W}(-H) = 0 \tag{B.2}$$

The inner and boundary dispersion relations are then:

$$\delta_z^2 - \frac{\epsilon_i^2\delta_x^2}{\omega^2} = 0 \tag{B.3a}$$

$$\omega^2 = \frac{\delta_x^2\ \tan(\delta_z)}{\delta_z} \tag{B.3b}$$

In the long wave-approximation ($\delta_z \rightarrow 0$), (B.3a) and (B.3b) are approximately given by ($\delta_z = \epsilon_i,\ \omega = \delta_x$) and tends to the shallow-water solution ($\delta_z = 0,\ \omega = \delta_x$) (SHW, Table 1) for a homogeneous ocean ($\epsilon_i \rightarrow 0$).

Non-hydrostatic & incompressible model. In an incompressible (non-hydrostatic) ocean, the propagation relation (17) in a uniformly stratified, incompressible ocean turns to:

$$\tilde{W}''(z) + kx^2\left(\frac{g}{D_0\ \omega} - 1\right)\tilde{W}(z) = 0 \tag{B.4}$$

associated to the surface and bottom boundary conditions:

$$\tilde{W}'(0) - \frac{gk_x^2}{\omega^2}\tilde{W}(0) = 0, \quad \tilde{W}(-H) = 0 \tag{B.5}$$

The inner and boundary dispersion relations are then:

$$\delta_x^2 + \delta_z^2 - \frac{\epsilon_i^2\delta_x^2}{\omega^2} = 0 \tag{B.6a}$$

$$\omega^2 = \frac{\delta_x^2\ \tan(\delta_z)}{\delta_z} \tag{B.6b}$$

In the long wave-approximation ($\delta_z \rightarrow 0$), (B.6a) and (B.6b) are approximately given by ($\delta_z = \delta_x + \epsilon_i^2,\ \omega = \delta_x$) and tends to the long-swell solution ($\delta_z = \delta_x,\ \omega = \delta_x$) (LSW, Table 1) in a homogeneous ocean ($\epsilon_i \rightarrow 0$).

Dispersion surfaces. Fig. B.1 shows the inner and boundary dispersion surfaces for an incompressible ocean under the assumptions of hydrotaticity (a) and non-hydrostaticity (b).

- Under the hydrostatic assumption, all wave solution have real, positive vertical number δ_z. Fig. B.1.(a) shows two types of solutions, MIM for $\delta_z \approx \pi$ and barotropic-like mode for small δ_z which converge to barotropic mode when $\epsilon_i \rightarrow 0$.
- Under the non-hydrostatic assumption, Fig. B.1.(b) shows also two types of solutions, MIM for $\delta_z \approx \pi$ and MSW for $\delta_z \in i\mathbb{R}$.

Appendix C. Analytical solutions and vertical profiles of vertical velocity under constant Brunt-Väisälä frequency

Analytical solutions. We define in Section 2 the vertical velocity profile $\widetilde{W}(z)$ for a constant and uniform Brunt-Väsälä frequency by

$$\widetilde{W}(z) = e^{-z/(2D_0)}F(z) = e^{-z/2D_0}\frac{\sin(k_z(H+z))}{\sin(k_zH)} \tag{C.1}$$

and a vertical pressure profile $\widetilde{p}(z)$

$$\widetilde{p}(z) = \frac{\Omega^2}{g^2k_x^2(1-(\Omega/(c_sk_x))^2)}\left(N_0^2\widetilde{W}(z) + g\widetilde{W}'(z)\right).$$

with $\frac{1}{D_0} = \frac{N_0^2}{g} + \frac{g}{c_s^2}$, and where, for a given horizontal wave-number k_x, k_z and Ω are solutions of the inner and boundary dispersion relations. Highly accurate approximations of them can be found in Table 5.

Note that by construction (and using the boundary dispersion relation), we have $\widetilde{W}(0) = \widetilde{p}(0) = 1$.

The real analytical solutions of Eqs. ((14a), (14b), (14c), (14d)) which satisfy the bottom and surface conditions ((15a), (15b)) are given by:

$$\eta(x,t) = \eta_0\cos(k_xx)\cos(\Omega t) \tag{C.2}$$

$$u(x,z,t) = \eta_0\frac{gk_x}{\Omega}\sin(k_xx)\sin(\Omega t)\frac{\hat{\rho}_h(0)}{\hat{\rho}_h(z)}\widetilde{p}(z) \tag{C.3}$$

$$w(x,z,t) = -\eta_0\Omega\cos(k_xx)\sin(\Omega t)\frac{\hat{\rho}_h(0)}{\hat{\rho}_h(z)}\widetilde{W}(z) \tag{C.4}$$

$$p(x,z,t) = \eta_0\ g\hat{\rho}_h(0)\cos(k_xx)\cos(\Omega t)\widetilde{p}(z) \tag{C.5}$$

$$\rho(x,z,t) = \eta_0\hat{\rho}_h(0)\cos(k_xx)\cos(\Omega t)\left(\frac{N_0^2}{g}\widetilde{W}(z) + \frac{g}{c_s^2}\widetilde{p}(z)\right) \tag{C.6}$$

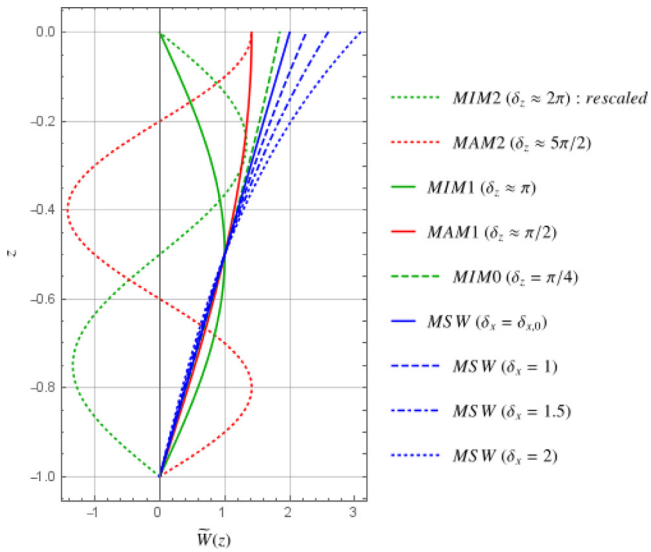

Fig. C.1. vertical profiles of vertical velocity $\widetilde{W}(z)$. Green curves: MIM solutions. Red curves: MAM solutions. Blue curves: MSW solutions.

with $\hat{\rho}_h(z) = \hat{\rho}_h(0)\, e^{-z/D_0}$ and η_0 a constant.

For an homogeneous $N_0^2 \to 0$ and incompressible ($c_s \to \infty$, and thus $D_0 \to \infty$) non hydrostatic ocean, the Airy's solutions are recovered (see e.g. Gill 1982, section 5.3). Indeed $k_z = ik_x, \Omega^2 = gk_x \tanh(Hk_x)$ and

$$\widetilde{W}_{\text{Airy}}(z) = F_{\text{Airy}}(z) = \frac{\sinh(k_x(H+z))}{\sinh(k_x H)},$$

$$\widetilde{p}_{\text{Airy}}(z) = \frac{\Omega^2}{gk_x^2}\widetilde{W}'_{\text{Airy}}(z) = \frac{\Omega^2}{gk_x}\frac{\cosh(k_x(H+z))}{\sinh(k_x H)},$$

leading to

$$\eta_{\text{Airy}}(x,t) = \eta_0 \cos(k_x x)\cos(\Omega t) \tag{C.7}$$

$$u_{\text{Airy}}(x,z,t) = \eta_0 \Omega \sin(k_x x)\sin(\Omega t)\frac{\cosh(k_x(H+z))}{\sinh(k_x H)} \tag{C.8}$$

$$w_{\text{Airy}}(x,z,t) = -\eta_0 \Omega \cos(k_x x)\sin(\Omega t)\frac{\sinh(k_x(H+z))}{\sinh(k_x H)} \tag{C.9}$$

$$p_{\text{Airy}}(x,z,t) = \hat{\rho}_h(0) g \eta_0 \cos(k_x x)\cos(\Omega t)\frac{\cosh(k_x(H+z))}{\cosh(k_x H)} \tag{C.10}$$

$$\rho_{\text{Airy}}(x,z,t) = 0 \tag{C.11}$$

Vertical profiles. Fig. C.1 shows the several vertical profiles of the vertical velocity for several propagating MSW, MIM-0 and MIM-1 solutions and vanishing MIM-0 solutions ($\omega^2 < 0$ and $\delta_x^2 < 0$).

For short-length MSW ($\delta_x > \delta_{x,0}$), the vertical profile of the vertical (blue curves) is concave, it is linear for $\delta_x = \delta_{x,0}$ and convex for long-waves ($\delta_x < \delta_{x,0}$). the vertical profiles of MIM-1 and MAM-1 (MIM-2 and MAM-2) show one (respectively two) extrema in the water column.

References

Apel, J.R., 1987. Principles of Ocean Physics. In: International Geophysics Series, Number v. 38, Academic Press, London, Orlando.

Auclair, F., Bordois, L., Dossmann, Y., Duhaut, T., Estournel, C., Floor, J., Marsaleix, P., Nguyen, C., Paci, A., Ulses, C., 2014. Implementation of a time-dependent bathymetry in a free-surface ocean model: Application to internal wave generation. Ocean Model. 80, 1–9.

Auclair, F., Bordois, L., Dossmann, Y., Duhaut, T., Paci, A., Ulses, C., Nguyen, C., 2018. A non-hydrostatic non-Boussinesq algorithm for free-surface ocean modelling. Ocean Model. 132, 12–29.

Auclair, F., Estournel, C., Floor, J.W., Herrmann, M., Nguyen, C., Marsaleix, P., 2011. A non-hydrostatic algorithm for free-surface ocean modelling. Ocean Model. 36 (1–2), 49–70.

Dossmann, Y., Auclair, F., Paci, A., 2013. Topographically induced internal solitary waves in a pycnocline: Primary generation and topographic control. Phys. Fluids 25 (6), 066601.

Dukowicz, J.K., 2013. Evaluation of various approximations in atmosphere and ocean modeling based on an exact treatment of gravity wave dispersion. Mon. Weather Rev. 141 (12), 4487–4506.

Eckart, C., 1960. Hydrodynamics of Oceans and Atmospheres. Pergamon Press.

Gill, A.E., 1982. Atmosphere-Ocean Dynamics. Academic Press Inc, San Diego.

Hilt, M., Auclair, F., Benshila, R., Bordois, L., Capet, X., Debreu, L., Dumas, F., Jullien, S., Lemarié, F., Marchesiello, P., Nguyen, C., Roblou, L., 2020. Numerical modelling of hydraulic control, solitary waves and primary instabilities in the Strait of Gibraltar. Ocean Model. 151, 101642.

Jensen, F.B., Kuperman, W.A., Porter, M.B., Schmidt, H., 2011. Computational ocean acoustics. Springer New York, New York, NY.

LeBlond, P.H., Mysak, L.A., 1981. Waves in the Ocean. Elsevier.

Lighthill, M.J., 1967. Waves in Fluids. Cambridge University Press.

Marchesiello, P., Auclair, F., Debreu, L., McWilliams, J., Almar, R., Benshila, R., Dumas, F., 2021. Tridimensional nonhydrostatic transient rip currents in a wave-resolving model. Ocean Model. 163, 101816.

Mei, C.C., Stiassnie, M., Yue, D.K.-P., 2005. Theory and Applications of Ocean Surface Waves: Linear Aspects. World Scientific.

Pedlosky, J., 2013. Geophysical Fluid Dynamics. Springer Science & Business Media.

Shchepetkin, A.F., McWilliams, J.C., 2005. The regional oceanic modeling system (ROMS): A split-explicit, free-surface, topography-following-coordinate oceanic model. Ocean Model. 9 (4), 347–404.

Skamarock, W.C., Klemp, J.B., Dudhia, J., 2001. Prototypes for the WRF (weather research and forecasting) model. In: Preprints, Ninth Conf. Mesoscale Processes, J11–J15. Amer. Meteorol. Soc., Fort Lauderdale, FL.

Smith, J.A., 2015. Revisiting oceanic acoustic gravity surface waves. J. Phys. Oceanogr. 45 (12), 2953–2958.

Tolstoy, I., 1963. The theory of waves in stratified fluids including the effects of gravity and rotation. Rev. Modern Phys. 35 (1), 207–230.